This document is the Submitted Manuscript version of a Published Work that appeared in final form in Faseb Journal, April, 2020.
Online version: https://faseb.onlinelibrary.wiley.com/doi/abs/10.1096/fj.201902113R
DOI: https://doi.org/10.1096/fj.201902113R

The M_2 muscarinic receptor, in association to M_1, regulates the neuromuscular PKA molecular dynamics

V. Cilleros-Mañé[1], L. Just-Borràs[1], M. Tomàs[1], N. Garcia[1]*, J. M. Tomàs[1]*, M.A. Lanuza[1]*

[1]Unitat d'Histologia i Neurobiologia (UHNEUROB). Departament de Ciències Mèdiques Bàsiques. Universitat Rovira i Virgili. c/ Sant Llorenç 21, 43201 Reus. Spain.

**M.A.L., J.M.T. and N.G. contributed equally.*

#Correspondence may be addressed to either of these authors:

Maria A. Lanuza: mariaangel.lanuza@urv.cat

Josep Tomàs: josepmaria.tomas@urv.cat

#For editorial communications, please send correspondence to:

Maria A. Lanuza

Unitat d'Histologia i Neurobiologia (UHNEUROB)

Facultat de Medicina i Ciències de la Salut, Universitat Rovira i Virgili.

c/ Sant Llorenç 21 (43201) Reus, Spain

Telephone: +34 977 759351

Email address: mariaangel.lanuza@urv.cat

ORCID

V. Cilleros-Mañé	0000-0001-5690-9932
L. Just-Borràs	0000-0003-0473-3730
M. Tomàs	0000-0002-4151-1697
N. Garcia	0000-0002-3401-8335
M. A. Lanuza	0000-0003-4795-4103
J. Tomàs	0000-0002-0406-0006

Running title

M_1 and M_2 mAChR modulate PKA

Abbreviations

ACh, acetylcholine; **AKAP150**, A kinase anchor protein 150; **AT**, atropine; **C**, catalytic subunit; **cAMP**, cyclic adenosine monophosphate; **co-IP**, co-immunoprecipitation; **CREB**, cAMP response element-binding; **Cα**, catalytic subunit isoform α; **Cβ**, catalytic subunit isoform β; **ExS**, extrasynaptic region; **H-89**, N-[2-((p-bromocinnamyl)amino)ethyl]-5-isoquinolinesulfonamide 2 HCl; **HRP**, horseradish peroxidase; **KO**, Knockout; **M_1**, muscarinic acetylcholine receptor 1 subtype; **M_2**, muscarinic acetylcholine receptor 2 subtype; **mAChR**, muscarinic acetylcholine receptor; **MET**, methoctramine; **nAChR**, nicotinic acetylcholine receptor; **NMJ**, neuromuscular junction; **PBS**, phosphate buffered saline; **PIR**, pirenzepine; **PKA**, protein kinase A; **PKC**, protein kinase C; **R**, regulatory subunit; **RIα**, regulatory type I subunit α; **RIβ**, regulatory type I subunit β; **RIIα**, regulatory type II subunit α; **RIIβ**, regulatory type II subunit β; **SEM**, standard error of the mean; **SNAP-25**, synaptosome-associated protein 25; **Stx**, syntaxin; **Syn**, synaptic region.

ABSTRACT

M_1 and M_2 presynaptic muscarinic receptor subtypes increase and decrease, respectively, neurotransmitter release at neuromuscular junctions. M_2 involves protein kinase A (PKA), although the muscarinic regulation to form and inactivate the PKA holoenzyme is unknown. Here, we show that M_2 signaling inhibits PKA by downregulating Cβ subunit, upregulating RIIα/β and liberating RIβ and RIIα to the cytosol. This promotes PKA holoenzyme formation and reduces the phosphorylation of the transmitter release target SNAP-25 and the gene regulator CREB. Instead, M_1 signaling, which is downregulated by M_2, opposes to M_2 by recruiting R subunits to the membrane. The M_1 and M_2 reciprocal actions are performed through the anchoring protein AKAP150 as a common node. Interestingly, M_2 modulation on protein expression needs M_1 signaling. Altogether, these results describe the dynamics of PKA subunits upon M_2 muscarinic signaling in basal and under presynaptic nerve activity, uncover a specific involvement of the M_1 receptor and reveal the M_1/M_2 balance to activate PKA to regulate neurotransmission. This provides a molecular mechanism to the PKA holoenzyme formation and inactivation which could be general to other synapses and cellular models.

Keywords

Neuromuscular junction; Muscarinic receptors; PKA; SNAP-25.

INTRODUCTION

Synapses use plastic mechanisms to adjust the strength of the neurotransmitter release to any situation. At the neuromuscular junction (NMJ), muscarinic acetylcholine receptors (mAChR) participate in synaptic plasticity as presynaptic autoreceptors sensing and controlling the release of ACh (1–4). The five subtypes of mAChR are classified by their downstream signaling pathway. M_1, M_3 and M_5 use the protein $G\alpha_{q/11}$ to activate phospholipase C and protein kinase C (PKC), whereas M_2 and M_4 use $G\alpha_{i/0}$ to inhibit adenylyl cyclase and protein kinase A (PKA) (5). Even though mammalian NMJ express all five mAChR subtypes (6), evidence shows that in the adult synapse mainly M_1 and M_2 orchestrate the muscarinic signaling, M_1 increasing ACh release whereas M_2 decreasing it (1, 4, 7).

The PKA pathway has been extensively implicated in synaptic plasticity (8, 9), facilitating the probability of release at many synapses (10–14). This includes the NMJ, where PKA constitutively promotes normal ACh release (15, 16). In part, PKA could enhance the release by phosphorylating the synaptosome-associated protein-25 (SNAP-25) at Thr^{138} (17, 18), which has never been investigated at the NMJ. SNAP-25 phosphorylation by PKA is necessary to maintain the release-ready and primed pool of vesicles (19). Thus, the PKA phosphorylation of SNAP-25 could be responsible for some effects of muscarinic signaling. In addition, mAChR-PKA role in synaptic plasticity could also be transduced through the cyclic adenosine monophosphate (cAMP) response element binding protein (CREB), a master regulator of gene expression, whose activity has been linked to synaptic plasticity at the NMJ as well as in the central nervous system (20, 21).

PKA exists as an inactive tetramer formed by two regulatory (R) and two catalytic (C) subunits which interact among a pseudosubstrate domain. When cAMP binds to the R subunits, the C subunits are liberated and their catalytic activity starts (22–24). Murine models express four R subunit isoforms (RIα, RIβ, RIIα, RIIβ) and two C subunit isoforms (Cα, Cβ); whereas the Cγ gene is only found in primates (25, 26). Cα and Cβ subunits display essentially the same activation properties whereas RIβ-containing holoenzymes show increased sensitivity to cAMP-evoked activation than RIα-containing holoenzymes (27). Also, although RII holoenzymes seem more prone to dissociate than

RI, probably due to structural differences, RI are more efficient than RII in inducing CREB response regardless of the C subunit (28–30).

R subunits are differently expressed across tissues and exert distinct roles in cell differentiation and growth control (31, 32). RIα and RIIα are widely expressed, RIβ is highly expressed in the nervous tissue and RIIβ in the adipose and hepatic tissues (31–34). Moreover, few studies have located RIα, RIIα and RIIβ at the synaptic area of the skeletal muscle (35–37). Besides cAMP activation and tissue expression, PKA is also regulated by subcellular targeting (38, 39). In particular, the translocation between cytosol and membrane of both PKA C (40) and R subunits (41, 42) regulates their activity. When inactive, most PKA are anchored by binding R subunits to scaffold proteins called A-kinase anchoring proteins (AKAPs). These AKAPs contribute to PKA specificity by recruiting the PKA holoenzyme to distinct subcellular compartments near specific substrates (43–45). R subunits differ in their subcellular localization, RI being found mainly in the cytosol, whereas RII to the particulate fraction, associated to the nuclei, nucleoli, Golgi complex and microtubules (33, 46). Additionally, PKA can also be regulated by changes in its concentration through synthesis and degradation (47, 48) and by crosstalk with the PKC pathway at the NMJ (16) as well as in other systems (47, 49–51) although the molecular signaling involved is unknown.

The present work characterizes at the NMJ how M_1 and M_2 muscarinic signaling regulates the protein expression, subcellular distribution and membrane-cytosol translocation of specific PKA subunits and whether this regulation extends to the phosphorylation of its targets SNAP-25 and CREB. The main results show that M_2 receptor reduces the Cβ protein level and increases the expression and liberation of R subunits to the cytosol, resulting in the decrease of CREB and SNAP-25 phosphorylation. The downregulation of Cβ also occurs under presynaptic nerve activity. Moreover, a balance M_1/M_2 in the regulation of the PKA is evidenced as some M_2-induced changes need the cooperation of M_1 receptor and also because M_1 receptor produces several changes which oppose to M_2 like recruiting RIα, RIβ and RIIα to the membrane fraction. Therefore, here we show that M_1 and M_2 muscarinic receptors cooperate at the NMJ to regulate the PKA subunit expression, translocation and activity on SNAP-25 and CREB phosphorylation. This would be relevant to better understand the molecular regulation of

mAChR-PKA signaling over the neurotransmitter release and synaptic plasticity mechanisms.

MATERIALS AND METHODS

Animal care

The animals were cared for in accordance with the European Community Council Directive guidelines for the humane treatment of laboratory animals. Adult Sprague-Dawley rats (40-80 days; Criffa, Barcelona, Spain; RRID:RGD_5508397) were euthanized for tissue harvest and analysis. At least three animals ($n \geq 3$) were used as biological replicates for every experiment detailed below. All animal work was approved by the Ethics Comitee of Animal Experimentation of the Universitat Rovira i Virgili.

Antibodies

The antibodies used for Western blotting and their dilution are listed in Table 1. These antibodies presented bands of the predicted molecular weight without near prominent unspecific bands. The anti-M_1 and anti-M_2 antibodies were tested by subcellular fractionation and antigen preincubation. The corresponding bands of these GPCRs were enriched in the membrane fraction, absent in the cytosolic fraction and antigen preincubation strongly reduced them. The specificity of anti-SNAP-25 antibody was carefully determined in Simó et al., 2019 and we tested the recognition of its cAMP-dependent phosphorylation by anti-pSNAP-25 Thr^{138} antibody with H-89.

Knock-out cell lines

Anti-PKA antibodies were validated against knockout lysates to guarantee discrimination between isoforms. We used the following CRISPR/Cas-9 knockout controls: Cα knockout 293T cell lysate (#NBP2-65840), Cβ knockout HeLa cell lysate (#NBP2-64806), RIα knockout 293T cell lysate (#NBP2-65698) and RIIα knockout HeLa cell lysate (#NBP2-65316).

Chemicals

Muscarinic inhibition. Pirenzepine dihydrochloride (Tocris): 10 mM stock and used at 10 μM. Methoctramine tetrahydrochloride (Sigma): 1 mM stock and used at 1 μM. Atropine (Sigma): 200 μM stock and used at 2 μM (1).

PKA inhibition. PKA activity was blocked with N-[2-((*p*-Bromocinnamyl)amino)ethyl]-5-isoquinolinesulfonamide dihydrochloride (H-89, Calbiochem). H-89 was made as 5 mM stock and used at 5 μM.

In the experiments involving nerve stimulation treatment, muscle contraction was blocked using μ-conotoxin GIIIB (#C-270, Alomone Labs Ltd, Jerusalem, Israel). This toxin selectively inhibits sarcolemmal voltage-dependent sodium channels (VDSCs) without affecting synaptic ACh release and has been used extensively for electrophysiology studies at the diaphragm (16, 53–55). It was supplied as lyophilised powder of >99% purity and used at 1.5 μM.

All chemicals were diluted in Ringer's solution and both control and drug-containing solutions contained 0.1% dimethyl sulfoxide (DMSO) as the vehicle.

Tissue dissection and treatment

Diaphragm muscles from adult Sprague-Dawley rats was dissected with special care to preserve phrenic nerve connectivity. Isolated nerve-muscle preparations were immersed in Ringer's solution (mM: NaCl 137, KCl 5, $CaCl_2$ 2, $MgSO_4$ 1, NaH_2PO_4 1, $NaHCO_3$ 12, glucose 12.1 and DMSO 0.1%), oxygenated with O_2:CO_2 (95:5) and maintained at 26ºC.

All treatments were performed *ex-vivo* on excised diaphragm muscles. The experimental design was pairwise: one hemidiaphragm underwent the treatment while the other served as its paired untreated control. Single-inhibitor treatments were applied for 60 minutes, a period which allows the comparison with previous studies in the same model (52, 56, 57). Double-inhibitor treatments were performed to study the implication of PKA in muscarinic signaling. In these, the treated hemidiaphragms were first preincubated for 30 minutes in Ringer solution containing H-89 and afterwards for further 30 minutes in Ringer solution containing H-89 plus the muscarinic inhibitor specified.

The controls of the doubly inhibited preparations were incubated for 60 minutes in Ringer solution containing H-89 to discard the effects of the PKA inhibitor.

Phrenic nerve stimulation

In some experiments, we studied the muscarinic signaling under the presence of centrifugal input i.e. with phrenic nerve stimulation (previously described in (58)). In these experiments, the diaphragm was stimulated through the phrenic nerve with a pulse generator (CIBERTEC Stimulator CS 20) linked to a stimulus isolation unit (CIBERTEC ISU 165). Visible contractions served to verify successful nerve dissection before applying the contraction blocker μ-conotoxin GIIIB. After the preincubation of μ-conotoxin GIIIB (30 minutes), phrenic nerves were stimulated at 1 Hz for 30 minutes, a protocol which allows the maintenance of tonic functions without depleting synaptic vesicles. To study muscarinic signaling, treated hemidiaphragm preparations contained muscarinic inhibitors during the preincubation and stimulation whereas control preparations did not contain muscarinic inhibitors.

Sample processing and fractionation

Whole cell lysates. After being treated as indicated, the muscles were immediately frozen in liquid nitrogen. Homogenization was performed with an overhead stirrer (VWR International, Clarksburg, MD) in ice-cold lysis buffer (in mM: NaCl 150, Tris-HCl 50 (pH 7.4), EDTA 1, NaF 50, PMSF 1, Na_3VO_4 1; NP-40 1%, Triton X-100 0.1% and protease inhibitor cocktail 1% (Sigma, Saint Louis, MO, USA)). Insoluble materials were removed with two centrifugations at 4ºC: 1000g for 10 minutes and 15000g for 20 minutes. The final supernatant contained the whole cell fraction lysate.

Membrane/cytosol fractionated lysates. Unlike whole cell lysates, for membrane-cytosol fractionation, we homogenized the samples immediately after treatment (without a freezing step) and with a detergent-free lysis buffer (in mM: NaCl 150, Tris-HCl 50 (pH 7.4), EDTA 1, NaF 50, PMSF 1, Na_3VO_4 1; and protease inhibitor cocktail 1%). Insoluble materials were removed by centrifugation at 1000g for 15 minutes at 4ºC. The resulting supernatant was further centrifuged at 130000g for 1 hour. The new supernatant corresponded to the cytosolic fraction while the pellet to the membrane fraction. The latter was resuspended in detergent-containing lysis buffer (see above). The purity of the

subcellular fractionation was validated by Western blotting of the fraction-specific proteins GAPDH for cytosol and Na^+/K^+-ATPase for membrane.

Synaptic/Extrasynaptic fractionated lysates. After treating the muscles, we separated the synaptic and extra-synaptic regions as indicated in Figure 6A and previously stated (59). We performed control experiments to check that our separation protocol was accurate by incubating some diaphragms with TRITC conjugated α-bungarotoxin and staining the nerves with an antibody against antineurofilament-200. We did not detect any nerve nor postsynaptic area in the extra-synaptic region. Once separated, synaptic and extra-synaptic regions were processed equally.

Western blotting

The protein content of the samples was determined by the DC protein assay (Bio-Rad, CA, USA). Sample volumes containing 30 µg of protein were loaded in an 8% SDS-PAGE gel (10% to detect SNAP-25), separated for 10 min at 90V and 60 min at 110V, and electrotransferred to PVDF membranes (Bio-Rad, CA, USA). Blocking solutions were TBST containing 5% nonfat dry milk or 5% BSA. The primary antibodies were incubated overnight at 4°C and the HRP-conjugated secondary antibodies for 1 hour. Chemiluminescence was revealed with an ECL kit (GE Healthcare Life Sciences, UK) and imagined with the ChemiDoc XRS+ Imaging System (Bio-Rad, CA, USA).

ImageJ software was used to calculate the optical density of the bands, always from the same immunoblot image. The values were normalized to (1) the background values and (2) the total protein transferred on the PVDF membranes, analyzed with Sypro Ruby protein blot stain, (Bio-Rad, CA, USA) (60). Ratios between the experimental and control were calculated from the same membrane image. All presented data derive from densitometry measurements made of 3-10 separate replicates, plotted against controls. For Western blot desing no blinding was performed. Data quantification was performed blindly.

Immunohistochemistry

The PKA Cβ subunit was localized at the NMJ of diaphragm and *levator auris longus* (LAL) muscles by immunohistochemistry with identical results. The thinness of

LAL muscles improved the imaging and analysis of NMJs. Whole muscle mounts were fixed with 4% paraformaldehyde for 30 minutes. After fixation, the muscles were rinsed with PBS and incubated in 0.1 M glycine in PBS. Afterwards, PBS supplemented with 1% Triton X-100 and 4% BSA was used for permeabilization and blockade of nonspecific binding. Then, muscles were incubated overnight at 4°C in a mixture of primary antibodies raised in different species (anti-Cβ subunit and anti-S100 to label Schwann cells) and then rinsed. The muscles were then incubated for four hours at room temperature in a mixture of appropriate secondary antibodies. AChRs were detected with α-BTX conjugated with TRITC. At least three muscles were used as negative controls and no cross-reaction was detected between antibodies. In some muscles, plastic embedded semithin sections (0.5 μm) were obtained for high-resolution immunofluorescence analysis of the neuromuscular junction molecules as previously described (61). Immunolabelled NMJs from the whole-mount muscles were viewed with a laser-scanning confocal microscope (Nikon TE2000-E). Special consideration was given to the possible contamination of one channel by another. In experiments involving negative controls, the photomultiplier tube gains and black levels were identical to those used for a labelled preparation made in parallel with the control preparations. Images were assembled using Adobe Photoshop software (Adobe Systems, San Jose, CA) and neither the contrast nor brightness were modified.

Co-Immunoprecipitation

Co-immunoprecipitation was performed with the Pierce Co-IP kit (Thermo Scientific, USA). Briefly, 5 μg of antibody were crosslinked to cyanogen bromide-activated resin with sodium cyanoborohydride ($NaBH_3CN$) for 1.5 hours. Afterwards, the beads were quenched with 1M Tris-HCl supplemented with $NaBH_3CN$ and washed multiple times to remove non-bound antibodies. Sample volumes were normalized to contain 250 μg of protein and were immobilized to the appropriate antibody-resin with a gentile end-over-end mixing overnight at 4ºC. Non-bound proteins were discarded through multiple washing steps and bait-prey complexes were eluted with a low-pH elution buffer and immediately neutralized 1M Tris pH 9.5. In parallel, we performed mock co-IPs to control antibody fragment co-elution (using PBS instead of sample) and to control unspecific protein binding to the beads (using PBS instead of antibody). The eluted complexes were evaluated by SDS-PAGE and Western blotting. None of the

negative controls showed immunoreactivity (see Results). The used antibodies (anti-Cα, anti-Cβ and anti-RIβ) were suitable for IP according to the manufacturer and did not interfere with bait-prey interaction as they were raised against the C-terminal tail of the proteins, which does not participate in R-C subunit interaction.

Statistical analysis

The sample size was calculated as described in (62). All experiments were carried out at least in triplicate and are representative of at least three separate experiments. The results are presented as ratios or percentages of treatment to control (mean ± SEM). Shapiro-Wilk test was used to test sample normality. Paired Student t-test or its non-parametric alternative Wilcoxon test were used to determine the statistical significance of the ratios (considered as p-value <0.05). The calculations were elaborated using R 3.4.3 statistical package.

RESULTS

M_2 inhibits M_1 protein levels

To study the interplay between mAChR subtypes, we asked whether the inhibition of M_1 and M_2 affected their own and mutual expression. Selective muscarinic inhibition was carried out with the M_1-inhibitor pirenzepine (PIR), the M_2-inhibitor methoctramine (MET) and the M_1/M_2 pan-inhibitor atropine (AT). Figure 1A shows that M_1 blockade did not affect the protein levels of any receptor (M_1: 0.8±0.1; M_2: 1.0±0.2). On the contrary, M_2 blockade increased the levels of M_1 receptor (1.7±0.2) without altering the own M_2 (1.0±0.1). This indicates that M_2 signaling constitutively reduces M_1 levels. Additionally, M_1/M_2 inhibition (AT) did not modify any receptor (M_1: 0.8±0.1; M_2: 1.0±0.1). The difference between the effects of MET and AT suggests that M_2 blockade needs M_1 mAChR activity. We also identified this M_2 regulation pattern dependent of M_1 active in other findings of this work involving PKA subunits regulation (see the following sections).

Muscarinic modulation of PKA catalytic and regulatory subunits protein levels.

To study the protein levels of the PKA C and R subunits, we selected the antibodies which showed high specificity for the corresponding protein at the predicted molecular weight (in kDa): Cα 40, Cβ 40, RIα 48, RIβ 51, RIIα 50 and RIIβ 53 in the rat diaphragm (Figure 2A–B) (63, 64). Antibody specificity was validated through knockout cell lysates (Figure 2A). The anti-Cα antibody was reactive against the control and Cβ-KO lysates but negative against the Cα-KO. Inversely, anti-Cβ antibody was reactive against the control and Cα-KO lysates but negative against the Cβ-KO. This confirmed that anti-Cα and -Cβ antibodies do not cross-react between C subunits. Regarding the anti-RIα and -RIIα antibodies, their ~50 kDa band was positive in the control, abolished in their respective KO cells and unaffected by the KO of the other R subunit. To our knowledge, no RIβ-KO and RIIβ-KO cells are commercially available to perform a similar validation on the corresponding antibodies. Alternatively, antibodies can be validated with cell lines which do not express the target protein. We found no detectable levels of RIβ and RIIβ in the 293T and HeLa cell lysates, consistent with reports of no

detectable expression in these cell lines (28) and minimal expression in comparable human tissues (32). Furthermore, multiple sequence alignment with Clustal2.1 indicated that the antigens of anti-RIβ and -RIIβ antibodies are identical to the corresponding subunits and disparate from the other PKA subunits. Some anti-R antibodies showed an unspecific 30 kDa band which did not correspond to the predicted molecular weight and was not affected by any KO.

Once the anti-PKA antibodies were validated, we studied whether muscarinic signaling regulates the protein levels of C and R subunits. M_1 inhibition (Figure 2C) decreased the protein levels of the regulatory subunit RIIβ (0.6±0.1), without affecting any other PKA subunit (Cα 1.2±0.1; Cβ 1.1±0.1; RIα 1.0±0.1; RIβ 1.2±0.2 and RIIα 1.3±0.1). This suggests that M_1 pathway could constitutively reduce PKA activity through the increase of RIIβ levels. M_2 inhibition (Figure 2D) caused a two-fold increase in Cβ (1.9±0.4) without altering Cα (1.2±0.1). In addition, M_2 blockade decreased the regulatory subunits RIIα (0.7±0.1) and RIIβ (0.7±0.1), but not RIα or RIβ (respectively: 1.0±0.02 and 1.1±0.2). The downregulation of Cβ and upregulation of RIIα and RIIβ is consistent with the well-known role of M_2 signaling as inhibitor of PKA activity. M_1/M_2 inhibition (Figure 2E) only reduced the protein levels of RIIβ (0.8±0.04), while the other subunits remained unchanged after the treatment (Cα: 1.1±0.1; Cβ: 1.0±0.1; RIα: 1.2±0.2; RIβ: 1.1±0.2 and RIIα: 1.0±0.1). RIIβ downregulation could be linked to the activity of both M_1 and M_2 subtypes, because their selective inhibition induced the same effect. Interestingly, the pan-inhibitor AT did not show the effect of MET on Cβ and RIIα. Similarly to the M_1 downregulation, this is another node where M_2 effect needs M_1 active. Finally, we also studied wether the muscarinic modulation of catalytic subunits in presence of cholinergic input from phrenic nerve (Figure 1F). Similarly to basal conditions, Cα levels remained unchanged after any treatment. However, Cβ levels increased after M_2 blockade (2.9±0.2) but not after M_1 or M_1/M_2 inhibition (respectively: 1.0±0.1; 1.2±0.1).

In summary, both M_1 and M_2 receptors constitutively promote increased levels of RIIβ protein, which suggests some impairment of PKA activity. In comparison with M_1, M_2 would further reduce PKA activity by decreasing Cβ and increasing RIIα, actions which need the activity of M_1.

Regulation of cytosol-membrane PKA subunits translocation by mAChR.

Because neurotransmission relies on membrane trafficking and PKA action is regulated by subcellular distribution, we next examined how muscarinic signaling redistributes the PKA subunits between the membrane and cytosol fraction. Figure 3 shows the percentage of each PKA subunit in the cytosol and membrane fraction before and after muscarinic blockade in the diaphragm muscle. Line plots represent the cytosol/total ratio (i.e. both control and treatment values defined as 100%) whereas bars represent the relative percentages (i.e. control defined as 100% and treatment calculated in relation to control); the last is only discussed when protein levels change. Additionally, all data were normalized to the total protein loaded. We used Na^+/K^+-ATPase and GAPDH as markers to confirm the purity of the subcellular fractionation. Na^+/K^+-ATPase and GAPDH were highly enriched in their fraction and essentially undetectable in the counter-wise. Both C subunits were predominantly located in the cytosol fraction (% cytosol/total: Cα 79.8±0.02; Cβ 78.7±1.6) although also identifiable in the membrane (Figures 3A–C). Muscarinic imbalance did not induce the translocation of any C subunit. Similarly, in basal conditions, all R subunits were predominantly found in the cytosol (% cytosol/total: RIα 74.7±3.2; RIβ 75.7±7.6; RIIα 57.8±4.4 and RIIβ 71.3±3.2; Figures 3A–C). In line with previous studies, we found RII type subunits more linked to the membrane fraction than RI type (33, 46). Contrary to C subunits, muscarinic signaling modulated the location of R subunits. Particularly, M_1 blockade translocated RIα, RIβ and RIIα from the membrane to the cytosol (% cytosol/total: RIα +7.4±2.7; RIβ +11.8±2.8; RIIα +11.9±4.8) (Figure 3A). Pirenzepine decreased RIIβ protein levels in the cytosol and membrane (% cytosol: –29.3±7.3; % membrane: –10.4±2.9) without changing the translocation ratio between these compartments (% cytosol/total –5.1±2.9). Conversely, M_2 blockade translocated RIβ and RIIα from the cytosol to the membrane (% cytosol/total; RIβ –9.5±4.5; RIIα –30.4±6.0) without affecting RIα and RIIβ (% cytosol/total; RIα –2.9±2.4; RIIβ –4.5±3.4) (Figure 3B). The treatment with the pan-inhibitor AT did not change any regulatory subunit position, suggesting that the operativity of both receptors is needed to accomplish the membrane-cytosol translocation events (Figure 3C).

After determining that muscarinic imbalance affects the association of PKA to the cytosol and membrane compartments, we wondered whether their anchor protein

AKAP150 could be involved because it participates in neuronal processes and muscarinic signaling (65). We used an anti-AKAP150 antibody which reacted with a unique band of the predicted 150 kDa molecular weight (Figure 4A). This antibody was raised against the peptide sequence corresponding to the amino acids 428–449 of rat AKAP150. Blasting this sequence against a rat database showed 100% identity with AKAP150 (Uniprot sequence P24587) whereas the other hits presented gaps, less than 60% identity and their molecular weight did not correspond to the observed band (40-86 kDa versus the observed 150 kDa). In the total fraction (Figure 4B), M_1 inhibition decreased AKAP150 protein levels (0.3±0.1) whereas M_2 inhibition increased them (1.4±0.2). Probably due to their balance, M_1/M_2 inhibition did not induce any change (1.1±0.2). When analyzing membrane and cytosol fractions, we found that AKAP150 is majorly located in the membrane in basal conditions (membrane/total: AKAP150 88.2%±6.3) (Figure 4C). In concordance with the previous results, the pirenzepine-induced decrease of RIα, RIβ and RIIα in the membrane fraction was accompanied by a significant decrease in its anchoring protein AKAP150 in the same fraction (% membrane: –67.1% ± 4.8). The methoctramine-induced increase in RIβ and RIIα protein levels in the membrane fraction was accompanied by a significant increase of AKAP150 in the same fraction (% membrane: +51.2±18.3). Finally, atropine did not change AKAP150 in the membrane fraction in concordance with the previous results in the total fraction (% membrane: +28.7±9.6).

In summary, mAChRs modulate the cytosol-membrane translocation of PKA regulatory rather than catalytic subunits. The constitutive action of M_1 receptor seems to recruit RIα, RIβ and RIIα to the membrane fraction whereas the constitutive effect of M_2 mAChR might inhibit the action of M_1 and release RIβ and RIIα to the cytosol, increasing the probability to assemble the holoenzyme. This balance involves the anchoring protein AKAP150, whose levels are regulated to recruit PKA subunits or release them to the cytosol.

M_2 regulates the interaction between synaptic-enriched PKA subunits

To further prove if the translocation of R subunits to the membrane was accompanied by a release of the cytosolic C subunits, we investigated their interaction

414 after M_2 inhibition (Figure 5). Due to the wide cellular and tissue distribution of PKA
415 subunits, we detected them in the synaptic (Syn) and extra-synaptic (ExS) regions (Figure
416 5A). We studied Cα and Cβ and focused on their relation with RIβ because (1) its levels
417 do not change after muscarinic inhibition, but (2) it translocates after treatment possibly
418 modulating the cytosolic C subunits and (3) it is specifically expressed in the nervous
419 system (31–34). Figure 5B shows that Cβ and RIβ are enriched in the synaptic area of
420 non-treated diaphragms (Cβ: 1 Syn; 0.6±0.1 ExS; RIβ: 1 Syn; 0.4±0.03 ExS) while Cα
421 was almost equally distributed between synaptic and extra-synaptic (Cα: 1 Syn;
422 0.96±0.02 ExS). In concordance with the results in the total lysate (see Figure 2), the
423 treatment with MET increased Cβ in both synaptic and extrasynaptic regions (Cβ:
424 +0.2±0.2 Syn+MET; +0.2±0.1 ExS+MET) without changing RIβ (RIβ: –0.09±0.1
425 Syn+MET; +0.01±0.1 ExS+MET).

426 Next, to precisely locate Cβ in the NMJ, we used fluorescent
427 immunohistochemistry and confocal microscopy. Plastic embedded semithin sections
428 (0.5 μm) were used for high-resolution immunofluorescence analysis of neuromuscular
429 junction molecules (61). Figure 5C shows a NMJ stained with triple labeling: Cβ in green,
430 AChRs in red, Schwann cells (S100) in blue. The PKA Cβ subunit label is clearly present
431 in granular form on the S100-positive teloglial cells. The muscle cell also presents a very
432 faint general labeling on the sarcoplasm, which is higher in a band (arrow) around 2 μm
433 below the AChR-delineated postsynaptic gutters. Also, remarkable Cβ labeling can be
434 observed in the space occupied by the nerve terminal between the blue S100 positive
435 Schwann cell and the red postsynaptic gutters (arrowhead). In conclusion, Cβ is present
436 in the three cell components of the neuromuscular synapse.

437 Co-immunoprecipitation of RIβ in the total lysate rescued both Cα and Cβ in the
438 diaphragm at basal conditions, indicating that RIβ interacts with the two C subtypes
439 (Figure 5D). Additionally, M_2 inhibition with MET decreased the ability of RIβ antibody
440 to rescue Cα and Cβ, indicating a weaker association between RIβ and Cα and Cβ. This
441 is in concordance with M_2 being a $G\alpha_{i/0}$-coupled GPCR, whose inhibition increases
442 cAMP and results in the disassembling of the PKA R:C holoenzyme. Because RIβ is
443 enriched at the synaptic region of the diaphragm, neuronally expressed, and its interaction
444 with C subunits is modulated by M_2, RIβ is one potential mediator of M_2 signaling to

445 modulate the PKA phosphorylation of SNAP-25 Thr^{138} (see next section) at nerve
446 terminals of the NMJ.

447

448 ***Muscarinic modulation of CREB and SNAP-25 phosphorylation by PKA.***

449 To complete the analysis of the mAChR-PKA coupling, we evaluated PKA
450 activity after each mAChR subtype inhibition by determining the phosphorylation of the
451 PKA substrates CREB and SNAP-25 (Figure 6A–F). CREB serine 133 (Ser^{133}) is a well-
452 known PKA target that regulates gene transcription. SNAP-25 is a SNARE component
453 that is crucial for neurotransmission and it is phosphorylated by PKA on threonine 138
454 (Thr^{138}).

455 Figure 6A shows that M_1 inhibition does not affect CREB protein level and
456 phosphorylation (pCREB: 1.1±0.2; CREB: 0.8±0.1). On the contrary, M_2 inhibition
457 increased the phosphorylation of CREB (1.4±0.2) without altering its protein levels
458 (0.9±0.1). This result indicates that M_2 inhibits CREB phosphorylation, probably by
459 reducing PKA phosphorylating activity. Additionally, the M_1/M_2 muscarinic inhibition
460 did not affect CREB phosphorylation (pCREB: 0.8±0.2; CREB: 1.0±0.2) further
461 indicating the need of the M_1. Moreover, to ensure that muscarinic action on CREB is
462 conveyed through PKA, we studied the effect of muscarinic inhibitors after PKA
463 blockade with H-89. H-89 is a cell-permeable, potent and reversible ATP-competitive
464 inhibitor of PKA (Ki = 48 nM). As expected, PKA downregulation with H-89 reduced
465 phospho-CREB level (Figure 6B; pCREB: 0.7±0.1; CREB: 1.0±0.2). Figure 6C shows
466 the previous incubation with H-89 abolishes the MET effect on pCREB (pCREB:
467 1.2±0.2; CREB: 1.0±0.1). This demonstrates that M_2 inhibition of pCREB requires PKA
468 activity. Moreover, after PKA blockade, PIR continued without affecting pCREB
469 (pCREB: 0.8±0.1; CREB: 1.1±0.2) and the same for AT (pCREB: 1.0±0.2; CREB:
470 1.1±0.3), which indicates that the absence of M_1 action on CREB is not modified by PKA
471 blockade.

472 Next, we measured the influence of muscarinic signaling on SNAP-25 Thr^{138}, a
473 protein involved in the NMJ neurotransmitter release. Similarly to CREB, Figure 6D
474 shows that M_1 inhibition does not affect pSNAP-25 Thr^{138} phosphorylation (pSNAP-25:
475 1.0±0.1; SNAP-25: 1.0±0.04). However, M_2 inhibition induced an increase in phospho-

476 SNAP-25 Thr^{138} (1.2±0.1) without altering its protein levels (0.8±0.05). Additionally,
477 M_1/M_2 inhibition did not affect SNAP-25 phosphorylation (pSNAP-25: 1.0±0.1; SNAP-
478 25: 1.1±0.1). We studied the effect of H-89 on SNAP-25 Thr^{138} phosphorylation and how
479 this inhibitor influenced muscarinic signaling. Figure 6E shows that H-89 reduces SNAP-
480 25 phosphorylation without affecting its protein level (pSNAP-25: 0.75±0.1; SNAP-25:
481 1.1±0.03). Finally, Figure 6F shows also that the MET effect on pSNAP-25 can be
482 abolished by a previous incubation with H-89, demonstrating that M_2 inhibition of
483 pSNAP-25 requires PKA activity (pSNAP-25: 1.1±0.7; SNAP-25: 1.0±0.04).

484

DISCUSSION

Since long time ago, PKA has been implicated in synaptic plasticity, enhancing the probability of release in the nerve terminal (8, 24, 66) as well as controlling the postsynaptic response (67–69). This kinase promotes ACh release at the NMJ, remarkably via the phosphorylation of the release machinery and its regulatory components (reviewed in Leenders and Sheng, 2005). At the NMJ, the M_2 mAChR subtype inhibits PKA through the reduction of cAMP levels, a mechanism which decreases ACh release (1, 7). However, the dynamics of PKA at the NMJ upon activation remain unknown. On the other hand, the M_1 subtype couples PKC isoforms to potentiate ACh release (1, 7) and PKA and PKC are also interconnected in regulating neurotransmitter release at the NMJ (16). In the present study we found how M_2 pathway regulates PKA subunit levels, translocation and interaction in the rat diaphragm to phosphorylate representative transmitter release targets, like SNAP-25, and the PKA-dependent CREB. Moreover, we demonstrate a crosstalk between M_1 and M_2 inhibition at the molecular level that would impact in the functionality of the NMJ. Figure 7A provides a summary of the main results.

M_1 and M_2 mutual influence

M_1 and M_2 muscarinic signaling pathways converge to antagonistically regulate ACh release at the NMJ: M_1 increases whereas M_2 decreases ACh release (7). Overall, M_2 signaling predominates over M_1, evidenced by M_1/M_2 inhibition increasing the quantal content similar to M_2 inhibition alone (1). Here, we found that M_2 decreases the protein levels of M_1, providing a molecular explanation to previous findings of M_2 overcoming functionaly M_1. The downregulation of M_1 protein levels by M_2 might be caused by internalization and degradation (70) or by a decrease in PKA/pCREB-induced synthesis (71). On the other hand, the downregulation of M_1 protein levels (and activity) by M_2 and not M_2 by M_1 might be due to different pathways of internalization and degradation. In particular, M_1 mAChR is internalized in a β-arrestin/dynamin dependent manner, whereas sequestration of M_2 is largely independent of these proteins (72, 73). Interestingly, we found that M_2 needs M_1 activity to reduce the own M_1 levels, because the effect does not happen when both receptors are blocked. This receptor downregulation could be linked to PKC, as downstream kinase of M_1 mAChR which promotes GPCR kinase (GRK) activity and β-arrestin/dynamin dependent internalization (74, 75). In fact,

517 we found that all the M_2-induced changes in PKA subunits expression and translocation
518 need non-blocked M_1 receptors, favoring the idea of a direct influence between M_1 and
519 M_2. Furthermore, the results showing that while M_2 inhibits activity (and protein levels)
520 of M_1, M_1 has no direct influence on M_2 could also be explained by a stronger tonic
521 activation of M_2 than M_1 receptors. The muscarinic signaling observed in this study could
522 be caused by the constitutive G protein-coupled receptors activity (76) or by the
523 spontaneous ACh release (77, 78).

524 ***Muscarinic modulation of PKA catalytic and regulatory subunits protein level***

525 Besides cAMP availability, PKA activity is also regulated by its concentration
526 through transcriptional or posttranscriptional changes in the synthesis or degradation of
527 its subunits (47, 67, 79). In this work, we found that both M_1–PKC and M_2–PKA
528 pathways regulate the protein levels and translocation of specific PKA subunits. The
529 unexpected role of M_1–PKC pathway could be related to the few studies finding that both
530 PKC and PKA activities can modify the expression of PKA subunits (particularly Cα and
531 RIIβ) in cultured cells (47, 80). Despite being generally considered G_q-specific, M_1 has
532 also been linked to PKA stimulation via G_s alpha subunit in cell cultures (81, 82) and
533 PKA and PKC are also interconnected in regulating neurotransmitter release at the NMJ
534 (16). For example, a cross-link between M_1 and M_2 pathways could be through a calcium-
535 induced reduction of cAMP (83, 84). However, the dynamics of PKA in NMJ upon
536 activation remained poorly understood. Regarding M_1 upregulation of RIIβ and M_2
537 downregulation of Cβ and upregulation of RIIα/β, both receptors could apparently be
538 associated to a decrease in PKA catalytic activity because increased turnover of C
539 subunits or elevated levels of R subunits results in reduced catalytic activity (48). The
540 downregulation of Cβ might affect the synaptic machinery, because Cβ is highly
541 expressed in the nervous system (85, 86) and we found it abundant in the synaptic region
542 of the diaphragm and present at the nerve terminal of the NMJ (and also in the other two
543 synaptic cell components) like SNAP-25 (52). Interestingly, we also found this M_2 effect
544 over the Cβ subunit when the phrenic nerve is stimulated. Both M_1 and M_2 increase RIIβ
545 levels, which is a link between M_1 and M_2 pathways that could inhibit PKA activity and
546 allowing M_1 to indirectly influence M_2 signaling. In addition, M_2 blockade also decreases
547 the regulatory subunit RIIα. This indicates that the two isoforms of RII are involved in
548 the muscarinic downregulation of the PKA activity. In addition, the regulation of Cβ by

549 M_2 also occurs in presence of cholinergic input from phrenic nerve, demonstrating a
550 general mechanism of regulation, both tonicaly and in physiological condition. In fact, it
551 has been described that constitutive activity of neurotransmitter GPCRs may provide a
552 tonic support for basal neuronal activity (reviewed by (76)). Here, we show that tonic and
553 activated muscarinic signaling largely modulates proteins responsible of regulating
554 synaptic transmission and plasticity, suggesting that the signaling pathway elicited by
555 muscarinic receptors works in transmission of NMJ. Interestingly, both Cβ and RIIα
556 changes by M_2 need M_1 activity, indicating the cooperation of both mAChR pathways to
557 control PKA activity. In summary, M_1 and M_2 receptors regulate the protein level of
558 several PKA subunits. This presumably reduces PKA activity as it has been described
559 that increased levels of R subunits reduce catalytic activity (48).

560 ***PKA subunits membrane-cytosol translocation is modulated by mAChR.***

561 The PKA distribution between the membrane and cytosolic compartments has
562 implications in their kinase activity and specificity (24, 41). In our model, C subunits are
563 mainly located in the cytosol and the presence of R subunits in the cytosol is required for
564 the negative regulation of the PKA catalytic activity. We detected that PKA Cα, Cβ and
565 RIα, RIβ and RIIβ subunits are mainly associated to the cytosol fraction (~75%
566 cytosol/total) and only RIIα had less presence in the cytosol (60%). This is consistent
567 with reports that PKA RI type is diffused in the cytoplasm of cells, whereas RII type is
568 usually associated to membrane compartments (33, 35, 41, 46) due to their higher affinity
569 to PKA-anchoring proteins (43). PKA activity can be regulated by cytosol/membrane
570 translocation of both C (40) and R subunits (41, 42). In the adult rat diaphragm, we found
571 that mAChR signaling regulates the translocation of PKA R subunits rather than C
572 subunits. Our results indicate that M_1 receptors constitutively recruit RIα, RIβ and RIIα
573 to the membrane whereas M_2 receptors liberate RIβ and RIIα to the cytosol. Also, the
574 absence of effect when both M_1 and M_2 are blocked with AT could be because their
575 opposed actions cancel each other out or, alternatively, because one subtype is necessary
576 for the other. We speculate that the coexistence of both mAChR subtypes may balance
577 the presence of RIβ and RIIα in the cytosol to finely control PKA C activity. RI subunits
578 are known to associate with membrane fractions when they are not associated with C
579 subunits (41). In this regard, a similar mechanism was proposed by Stefan *et al.,* 2011
580 (42), where a GPCR-mediated cAMP elevation promotes dissociation of the PKA

heterotetramer and recruitment of R subunits to $G\alpha_{i/0}$ proteins at the membrane. Thus, the recruitment to the membrane of RIβ and RIIα produced by the M_2 inhibitor methoctramine could be linked with the increase in cAMP produced by the inhibitor. Also, the eventual prevalence of M_2 downstream signaling in basal conditions at the NMJ (1) as well as the M_2-induced decrease of M_1 would promote the release and presence of R subunits in the cytosol. The close association of the regulatory and catalytic subunits prevents the phosphorylating activity of the catalytic ones (Reviewed in (24)), and we show that M_2 signaling tonically maintains RIβ strongly associated with Cβ and Cα at the synaptic areas of the skeletal muscle. Further experiments about the interaction between subunits will be needed to better understand the mechanism of inhibition of the C subunit by the R ones.

Therefore, M_1 receptor constitutively maintains PKA RIα, RIβ and RIIα in the membrane fraction whereas the tonic effect of M_2 mAChR might inhibit the action of M_1, enhancing the release of PKA RIβ and RIIα to the cytosol. This mAChR-modulated balance of the membrane-cytosol position of these subunits involves a mechanism that include the anchoring protein AKAP150 and may be relevant in PKA activity regulation and specificity. The mechanisms that regulate AKAP150 expression and degradation remain unclear. Here we demonstrate that M_1 mAChR, known to potentiate ACh release, upregulates AKAP150. Contrarily, we found that M_2 mAChR downregulates AKAP150. Changes in AKAP150 expression have been determined in other systems (87–89). In particular, impaired Ca^{2+} cycling in a heart failure model (89) or induced by PIR (our results) has been linked to AKAP150 downregulation. On the other hand, exercise training in rats (87) and ACh release upregulation by MET (our results) increases AKAP150 indicating that M_1 can increase the association PKA R subunits to the membrane, thus increasing the cytosolic activity of C subunits. Targeting of PKA to specific sites within the cell is largely achieved by AKAPs (43, 90). Also, R translocation to the membrane aside from AKAP150 could also been related to $G\alpha_{i/0}$ association (42). Additionally, AKAP150 has been shown to be also an anchoring protein for PKC (91–93) and it could be possible that the M_1 upregulation of AKAP150 affects PKC contributing thus to the functional and molecular relation between PKC and PKA to regulate neurotransmission at the NMJ. It is stimulating to think that multi-protein complexes orchestrated by AKAPs create presynaptic membrane sites wherein signalling pathways converge and are regulated to optimizate the functionality of the NMJ.

614

615 ***M_2 inhibits PKA activity on CREB and SNAP-25 phosphorylation***

616 PKA phosphorylates many molecular targets related with immediate transmitter
617 release or with long-lasting regulation of neurotransmission. Some PKA targets directly
618 involved in transmitter release are α-SNAP (94), CSP (95), synapsin I (96), Snapin (97),
619 syntaphilin (98), rabphilin (99), RIM1 (100), and SNAP-25 (17, 18). SNAP-25, together
620 with synaptobrevin and syntaxin are the three SNARE proteins of the core fusion vesicle
621 complex, which is involved in vesicle docking, priming and triggering fast exocytosis
622 (101, 102). It has been proposed that PKA phosphorylation of SNAP-25 at Thr^{138} controls
623 the size of the releasable vesicle pools, whereas the novel PKCε phosphorylation of
624 SNAP-25 at Ser^{187} is involved in regulating refilling after the pools have been emptied
625 (9, 52, 103). Here we found that M_1 inhibition does not affect SNAP-25 Thr^{138}
626 phosphorylation but M_2 inhibition induced an important increase which can be abolished
627 by a previous incubation with H-89, demonstrating that M_2 inhibition of pSNAP-25
628 involves the modulation of the PKA activity.

629 CREB is a long-lasting master regulator of gene expression, whose activity has
630 been linked to synaptic plasticity at the NMJ as well as in the central nervous system (20).
631 CREB is phosphorylated by various kinases, for instance cAMP/PKA, ERK1/2, and
632 PI3K/Akt (reviewed by (9, 104)) and we selectively analyzed the PKA/CREB signaling
633 pathway. Similarly to SNAP-25 phosphorylation, M_1 inhibition does not affect CREB
634 phosphorylation but M_2 inhibition increased it indicating that M_2 normally inhibits PKA
635 phosphorylating activity on CREB. The M_2 inhibition effect on pCREB can be markedly
636 reduced by a previous incubation with H-89, indicating that M_2 inhibition of pCREB
637 requires PKA activity. Our ex-vivo approach maintains the architecture of synapses as
638 the in vivo conditions and allows to study an accurate version of the behavior and function
639 of the neuromuscular system. However, PKA is widely expressed and some mechanisms
640 described here could occur in different cell types. For example, CREB expression and
641 phosphorylation at the skeletal muscle occurs in nuclei of myocytes and is differentially
642 activated in synaptic and extra-synaptic regions of fast- and slow-twitch muscles (21).

643 The mAChR M_1 and M_2 subtypes are present at the nerve terminal but also at the
644 perisynaptic glial cell (6), suggesting that mAChR signaling could be initiated in both

cells (Figure 7B–C). However, although it has been demonstrated the presence of mAChR in rat cultured skeletal muscle membrane and developing muscle fibers, the innervated adult skeletal myocytes do not express mAChRs (105–108). Therefore, in case that some of the mAChR effects on PKA subunits and/or the phosphorylation of its targets might occur in the postsynaptic cell, it would be an evidence of the communication between cells through the signaling and indicate the complexity of the mAChR regulation (Figure 7D). Stabilization of the nAChR at the postsynaptic membrane is related with PKA activity (109–113) and in particular by the RIα subunit (36, 114, 115) and we could think that this mechanism might be anterogradely regulated by mAChR signaling.

The block of both M_1 and M_2 receptors with AT did not affect SNAP-25 and CREB phosphorylation indicating that M_2 needs M_1 operativity. M_1 modulates also the translocation to the membrane of several R subunits and the protein level of RIIβ though without consequences in CREB and SNAP-25 phosphorylation. This suggests that the M_2 inhibition of Cβ and translocation of R subunits to the cytosol could be responsible for the reduced phosphorylation of SNAP-25 and CREB although needs M_1 active.

Concluding remarks

It is known that the activation of M_2 subtype mAChR begins a Gi protein coupled downstream signal that inhibits adenylyl cyclase, cAMP levels and PKA activity with the subsequent decrease in ACh release at the NMJ. In the present work, we determined the dynamics of PKA subunits at the NMJ providing a molecular mechanism of the PKA holoenzyme formation and inactivation upon constitutive and activated muscarinic signaling that could be general to other synapses and cellular models. The M_2 action reduces the Cβ protein level, increases RIIα and RIIβ, and translocates RIβ and RIIα to the cytosol with the involvement of the anchoring protein AKAP150. This coincides with a decrease in the phosphorylation level of the master regulator of gene expression CREB and SNAP-25 that are PKA targets and with a decrease in the neurotransmission (1). Some of the M_2-induced changes need an active M_1 receptor (reduction of the Cβ and increase of the RIIα) while some other M_2-induced change can be additionally produced also by M_1 receptor action (the increase of the RIIβ protein and their release to the cytosol). On the other hand, M_1 receptor seems to produce several changes that would be interpreted as opposed to M_2 by holding RIα, RIβ and RIIα in the membrane fraction. Reciprocally, M_2 reduces M_1 protein level. Altogether, these results reveal the complexity

677 of PKA expression and regulation by muscarinic signaling and points to the operation of
678 a balance M_1/M_2 in the regulation of the PKA activation. At the nerve terminal of the
679 NMJ, the tonic action of the M_2 receptor would stabilize the holoenzymes formed by Cα
680 and Cβ with at least RIβ. This coincides with the final reduction in the phosphorylation
681 level of the essential exocytotic protein SNAP-25.

Acknowledgments

This work was funded by a grant from the Ministerio de Economía y Competitividad (MINECO), the Agencia Estatal de Investigación (AEI) and the European Regional Development Fund (ERDF) (SAF2015-67143-P); a grant from the Universitat Rovira i Virgili (URV) (2014PFR-URV-B2-83 and 2017PFR-URV-B2-85); and a grant from the Catalan Government (2014SGR344 and 2017SGR704). V.C. was supported by a grant from MINECO under the framework of the Sistema Nacional de Garantía Juvenil, the European Social Fund (ESF) and the Iniciativa de Empleo Juvenil (IEJ) reference code: LE1511314-2014PEJ-04.

Author Contributions

N.G., J.M.T., M.A.L designed research; V.C., L.J. performed research; V.C., L.J., M.T., N.G., J.M.T., M.A.L analyzed data. V.C., L.J., J.M.T., M.A.L wrote the paper. All authors read and approved the final version.

Competing interests

The authors declare no competing financial interests.

Ethics Statement

The animals were cared for in accordance with the guidelines of the European Community Council Directive of 24 November 1986 (86/609/EEC) for the humane treatment of laboratory animals. All the procedures realized were revised and authorized by the Animal Research Committee of the Universitat Rovira i Virgili (Reference number: 0289).

REFERENCES

1. Santafé, M. M., Lanuza, M. A., Garcia, N., Tomàs, M., and Tomàs, J. M. (2007) Coupling of presynaptic muscarinic autoreceptors to serine kinases in low and high release conditions on the rat motor nerve terminal. *Neuroscience* **148**, 432–440

2. Minic, J., Molgó, J., Karlsson, E., and Krejci, E. (2002) Regulation of acetylcholine release by muscarinic receptors at the mouse neuromuscular junction depends on the activity of acetylcholinesterase. *Eur. J. Neurosci.* **15**, 439–448

3. Slutsky, I., Silman, I., Parnas, I., and Parnas, H. (2001) Presynaptic M_2 muscarinic receptors are involved in controlling the kinetics of ACh release at the frog neuromuscular junction. *J. Physiol.* **536**, 717–725

4. Slutsky, I., Parnas, H., and Parnas, I. (1999) Presynaptic effects of muscarine on ACh release at the frog neuromuscular junction. *J. Physiol.* **514**, 769–782

5. Caulfield, M. P. (1993) Muscarinic receptors - characterization, coupling and function. *Pharmacol. Ther.* **58**, 319–379

6. Garcia, N., Santafé, M. M., Salon, I., Lanuza, M. A., and Tomàs, J. (2005) Expression of muscarinic acetylcholine receptors (M1-, M2-, M3- and M4-type) in the neuromuscular junction of the newborn and adult rat. *Histol. Histopathol.* **20**, 733–743

7. Santafé, M. M., Salon, I., Garcia, N., Lanuza, M. A., Uchitel, O. D., and Tomàs, J. (2003) Modulation of ACh release by presynaptic muscarinic autoreceptors in the neuromuscular junction of the newborn and adult rat. *Eur. J. Neurosci.* **17**, 119–127

8. Nguyen, P. V. and Woo, N. H. (2003) Regulation of hippocampal synaptic plasticity by cyclic AMP-dependent protein kinases. *Prog. Neurobiol.* **71**, 401–437

9. Leenders, A. G. M. and Sheng, Z.-H. (2005) Modulation of neurotransmitter release by the second messenger-activated protein kinases: implications for presynaptic plasticity. *Pharmacol. Ther.* **105**, 69–84

10. Dixon, D. and Atwood, H. (1989) Adenylate cyclase system is essential for long-term facilitation at the crayfish neuromuscular junction. *J. Neurosci.* **9**, 4246–4252

11. Chavez-Noriega, L. and Stevens, C. (1994) Increased transmitter release at excitatory synapses produced by direct activation of adenylate cyclase in rat hippocampal slices. *J. Neurosci.* **14**, 310–317

12. Klein, M. (1994) Synaptic augmentation by 5-HT at rested aplysia sensorimotor synapses: Independence of action potential prolongation. *Neuron* **13**, 159–166

13. Weisskopf, M., Castillo, P., Zalutsky, R., and Nicoll, R. (1994) Mediation of hippocampal mossy fiber long-term potentiation by cyclic AMP. *Science (80-.).* **265**, 1878–1882

14. Trudeau, L.-E., Emery, D. G., and Haydon, P. G. (1996) Direct Modulation of the Secretory Machinery Underlies PKA-Dependent Synaptic Facilitation in Hippocampal Neurons. *Neuron* **17**, 789–797

15. Santafé, M. M., Lanuza, M. A., Garcia, N., and Tomàs, J. (2006) Muscarinic autoreceptors modulate transmitter release through protein kinase C and protein kinase A in the rat motor nerve terminal. *Eur. J. Neurosci.* **23**, 2048–2056

16. Santafé, M. M., Garcia, N., Lanuza, M. A., Tomàs, M., and Tomàs, J. (2009) Interaction between protein kinase C and protein kinase A can modulate transmitter release at the rat neuromuscular synapse. *J. Neurosci. Res.* **87**, 683–690

17. Risinger, C. and Bennett, M. K. (1999) Differential Phosphorylation of Syntaxin and Synaptosome-Associated Protein of 25 kDa (SNAP-25) Isoforms. *J. Neurochem.* **72**, 614–624

18. Hepp, R., Cabaniols, J.-P., and Roche, P. A. (2002) Differential phosphorylation of SNAP-25 in vivo by protein kinase C and protein kinase A. *FEBS Lett.* **532**, 52–56

19. Nagy, G., Reim, K., Matti, U., Brose, N., Binz, T., Rettig, J., Neher, E., and Sørensen, J. B. (2004) Regulation of Releasable Vesicle Pool Sizes by Protein Kinase A-Dependent Phosphorylation of SNAP-25. *Neuron* **41**, 417–429

20. Kaplan, A. P., Keenan, T., Scott, R., Zhou, X., Bourchouladze, R., McRiner, A. J., Wilson, M. E., Romashko, D., Miller, R., Bletsch, M., Anderson, G., Stanley, J., Zhang, A., Lee, D., and Nikpur, J. (2017) Identification of 5-(1-Methyl-5-(trifluoromethyl)-1 H -pyrazol-3-yl)thiophene-2-Carboxamides as Novel and

765 Selective Monoamine Oxidase B Inhibitors Used to Improve Memory and
766 Cognition. *ACS Chem. Neurosci.* **8**, 2746–2758

767 21. Choi, R. C. Y., Chen, V. P., Luk, W. K. W., Yung, A. W. Y., Ng, A. H. M., Dong,
768 T. T. X., and Tsim, K. W. K. (2013) Expression of cAMP-responsive element
769 binding proteins (CREBs) in fast- and slow-twitch muscles: A signaling pathway
770 to account for the synaptic expression of collagen-tailed subunit (ColQ) of
771 acetylcholinesterase at the rat neuromuscular junction. *Chem. Biol. Interact.* **203**,
772 282–286

773 22. Walsh, D. A., Perkins, J. P., and Krebs, E. G. (1968) An adenosine 3',5'-
774 monophosphate-dependant protein kinase from rabbit skeletal muscle. *J. Biol.*
775 *Chem.* **243**, 3763–3765

776 23. Beavo, J. A., Bechtel, P. J., and Krebs, E. G. (1975) Mechanisms of control for
777 cAMP-dependent protein kinase from skeletal muscle. *Adv. Cyclic Nucleotide Res.*
778 **5**, 241–251

779 24. Taylor, S. S., Ilouz, R., Zhang, P., and Kornev, A. P. (2012) Assembly of allosteric
780 macromolecular switches: lessons from PKA. *Nat. Rev. Mol. Cell Biol.* **13**, 646–
781 658

782 25. Beebe, S. J., Øyen, O., Sandberg, M., Frøysa, A., Hansson, V., and Jahnsen, T.
783 (1990) Molecular Cloning of a Tissue-Specific Protein Kinase (C γ) from Human
784 Testis—Representing a Third Isoform for the Catalytic Subunit of cAMP-
785 Dependent Protein Kinase. *Mol. Endocrinol.* **4**, 465–475

786 26. Reinton, N., Haugen, T. B., Ørstavik, S., Skålhegg, B. S., Hansson, V., Jahnsen,
787 T., and Taskén, K. (1998) The Gene Encoding the Cγ Catalytic Subunit of cAMP-
788 Dependent Protein Kinase Is a Transcribed Retroposon. *Genomics* **49**, 290–297

789 27. Cadd, G. G., Uhler, M. D., and McKnight, G. S. (1990) Holoenzymes of cAMP-
790 dependent protein kinase containing the neural form of type I regulatory subunit
791 have an increased sensitivity to cyclic nucleotides. *J. Biol. Chem.* **265**, 19502–
792 19506

793 28. Stakkestad, Ø., Larsen, A. C. V, Kvissel, A.-K., Eikvar, S., Ørstavik, S., and
794 Skålhegg, B. S. (2011) Protein kinase A type I activates a CRE-element more

efficiently than protein kinase A type II regardless of C subunit isoform. *BMC Biochem.* **12**, 7

29. Prinz, A., Diskar, M., Erlbruch, A., and Herberg, F. W. (2006) Novel, isotype-specific sensors for protein kinase A subunit interaction based on bioluminescence resonance energy transfer (BRET). *Cell. Signal.* **18**, 1616–1625

30. Vigil, D., Blumenthal, D. K., Brown, S., Taylor, S. S., and Trewhella, J. (2004) Differential Effects of Substrate on Type I and Type II PKA Holoenzyme Dissociation. *Biochemistry* **43**, 5629–5636

31. Skålhegg, B. S. and Tasken, K. (2000) Specificity in the cAMP/PKA signaling pathway. Differential expression, regulation, and subcellular localization of subunits of PKA. *Front. Biosci.* **5**, d678-693

32. Fagerberg, L., Hallström, B. M., Oksvold, P., Kampf, C., Djureinovic, D., Odeberg, J., Habuka, M., Tahmasebpoor, S., Danielsson, A., Edlund, K., Asplund, A., Sjöstedt, E., Lundberg, E., Szigyarto, C. A.-K., Skogs, M., Takanen, J. O., Berling, H., Tegel, H., Mulder, J., Nilsson, P., Schwenk, J. M., Lindskog, C., Danielsson, F., Mardinoglu, A., Sivertsson, Å., von Feilitzen, K., Forsberg, M., Zwahlen, M., Olsson, I., Navani, S., Huss, M., Nielsen, J., Ponten, F., and Uhlén, M. (2014) Analysis of the Human Tissue-specific Expression by Genome-wide Integration of Transcriptomics and Antibody-based Proteomics. *Mol. Cell. Proteomics* **13**, 397–406

33. Brandon, E. P., Idzerda, R. L., and McKnight, G. S. (1997) PKA isoforms, neural pathways, and behaviour: making the connection. *Curr. Opin. Neurobiol.* **7**, 397–403

34. Cadd, G. and Stanley McKnight, G. (1989) Distinct patterns of cAMP-dependent protein kinase gene expression in mouse brain. *Neuron* **3**, 71–79

35. Perkins, G. A., Wang, L., Huang, L. J., Humphries, K., Yao, V. J., Martone, M., Deerinck, T. J., Barraclough, D. M., Violin, J. D., Smith, D., Newton, A., Scott, J. D., Taylor, S. S., and Ellisman, M. H. (2001) PKA, PKC, and AKAP localization in and around the neuromuscular junction. *BMC Neurosci.* **2**, 17

36. Röder, I. V., Choi, K.-R., Reischl, M., Petersen, Y., Diefenbacher, M. E., Zaccolo,

M., Pozzan, T., and Rudolf, R. (2010) Myosin Va cooperates with PKA RI to mediate maintenance of the endplate in vivo. *Proc. Natl. Acad. Sci.* **107**, 2031–2036

37. Xu, Z., Feng, X., Dong, J., Wang, Z.-M., Lee, J., Furdui, C., Files, D. C., Beavers, K. M., Kritchevsky, S., Milligan, C., Jin, J.-P., Delbono, O., and Zhang, T. (2017) Cardiac troponin T and fast skeletal muscle denervation in ageing. *J. Cachexia. Sarcopenia Muscle* **8**, 808–823

38. Gervasi, N., Hepp, R., Tricoire, L., Zhang, J., Lambolez, B., Paupardin-Tritsch, D., and Vincent, P. (2007) Dynamics of Protein Kinase A Signaling at the Membrane, in the Cytosol, and in the Nucleus of Neurons in Mouse Brain Slices. *J. Neurosci.* **27**, 2744–2750

39. Constantinescu, A., Gordon, A. S., and Diamond, I. (2002) cAMP-dependent Protein Kinase Types I and II Differentially Regulate cAMP Response Element-mediated Gene Expression. *J. Biol. Chem.* **277**, 18810–18816

40. Tillo, S. E., Xiong, W.-H., Takahashi, M., Miao, S., Andrade, A. L., Fortin, D. A., Yang, G., Qin, M., Smoody, B. F., Stork, P. J. S., and Zhong, H. (2017) Liberated PKA Catalytic Subunits Associate with the Membrane via Myristoylation to Preferentially Phosphorylate Membrane Substrates. *Cell Rep.* **19**, 617–629

41. Reinitz, C. A., Bianco, R. A., and Shabb, J. B. (1997) Compartmentation of the Type I Regulatory Subunit of cAMP-Dependent Protein Kinase in Cardiac Ventricular Muscle. *Arch. Biochem. Biophys.* **348**, 391–402

42. Stefan, E., Malleshaiah, M. K., Breton, B., Ear, P. H., Bachmann, V., Beyermann, M., Bouvier, M., and Michnick, S. W. (2011) PKA regulatory subunits mediate synergy among conserved G-protein-coupled receptor cascades. *Nat. Commun.* **2**, 598

43. Wong, W. and Scott, J. D. (2004) AKAP signalling complexes: focal points in space and time. *Nat. Rev. Mol. Cell Biol.* **5**, 959–970

44. Lohmann, S. M., DeCamilli, P., Einig, I., and Walter, U. (1984) High-affinity binding of the regulatory subunit (RII) of cAMP-dependent protein kinase to microtubule-associated and other cellular proteins. *Proc. Natl. Acad. Sci. U. S. A.*

81, 6723–6727

45. Scott, J. D. and Pawson, T. (2009) Cell Signaling in Space and Time: Where Proteins Come Together and When They're Apart. *Science (80-.).* **326**, 1220–1224

46. Keryer, G., Skålhegg, B. S., Landmark, B. F., Hansson, V., Jahnsen, T., and Taskén, K. (1999) Differential Localization of Protein Kinase A Type II Isozymes in the Golgi–Centrosomal Area. *Exp. Cell Res.* **249**, 131–146

47. Garrel, G., Delahaye, R., Hemmings, B. A., and Counis, R. (1995) Modulation of regulatory and catalytic subunit levels of cAMP-dependent protein kinase A in anterior pituitary cells in response to direct activation of protein kinases A and C or after GnRH stimulation. *Neuroendocrinology* **62**, 514–522

48. Spaulding, S. W. (1993) The ways in which hormones change cyclic adenosine 3', 5'-monophosphate-dependent protein kinase subunits, and how such changes affect cell behavior. *Endocr. Rev.* **14**, 632–650

49. Barnes, S. J. and Conn, P. M. (1993) Cholera toxin and dibutyryl cyclic adenosine 3',5'-monophosphate sensitize gonadotropin-releasing hormone-stimulated inositol phosphate production to inhibition in protein kinase-C (PKC)-depleted cells: evidence for cross-talk between a cholera toxin-sens. *Endocrinology* **133**, 2756–2760

50. Summers, S. T. and Cronin, M. J. (1986) Phorbol esters enhance basal and stimulated adenylate cyclase activity in a pituitary cell line. *Biochem. Biophys. Res. Commun.* **135**, 276–281

51. Cronin, M. J., Zysk, J. R., and Baertschi, A. J. (1986) Protein kinase C potentiates corticotropin releasing factor stimulated cyclic AMP in pituitary. *Peptides* **7**, 935–938

52. Simó, A., Cilleros-Mañé, V., Just-Borràs, L., Hurtado, E., Nadal, L., Tomàs, M., Garcia, N., Lanuza, M. A., and Tomàs, J. (2019) nPKCε Mediates SNAP-25 Phosphorylation of Ser-187 in Basal Conditions and After Synaptic Activity at the Neuromuscular Junction. *Mol. Neurobiol.*

53. Favreau, P., Le Gall, F., Benoit, E., and Molgó, J. (1999) A review on conotoxins targeting ion channels and acetylcholine receptors of the vertebrate neuromuscular

junction. *Acta Physiol. Pharmacol. Ther. Latinoam.* **49**, 257–267

54. Santafé, M. M., Garcia, N., Lanuza, M. A., Uchitel, O. D., and Tomás, J. (2001) Calcium channels coupled to neurotransmitter release at dually innervated neuromuscular junctions in the newborn rat. *Neuroscience* **102**, 697–708

55. Mantilla, C. B., Stowe, J. M., Sieck, D. C., Ermilov, L. G., Greising, S. M., Zhang, C., Shokat, K. M., and Sieck, G. C. (2014) TrkB kinase activity maintains synaptic function and structural integrity at adult neuromuscular junctions. *J. Appl. Physiol.* **117**, 910–920

56. Hurtado, E., Cilleros, V., Nadal, L., Simó, A., Obis, T., Garcia, N., Santafé, M. M., Tomàs, M., Halievski, K., Jordan, C. L., Lanuza, M. a., and Tomàs, J. (2017) Muscle Contraction Regulates BDNF/TrkB Signaling to Modulate Synaptic Function through Presynaptic cPKCα and cPKCβI. *Front. Mol. Neurosci.* **10**, 1–22

57. Obis, T., Hurtado, E., Nadal, L., Tomàs, M., Priego, M., Simon, A., Garcia, N., Santafé, M. M., Lanuza, M. A., and Tomàs, J. (2015) The novel protein kinase C epsilon isoform modulates acetylcholine release in the rat neuromuscular junction. *Mol. Brain* **8**, 80

58. Simó, A., Just-Borràs, L., Cilleros-Mañé, V., Hurtado, E., Nadal, L., Tomàs, M., Garcia, N., Lanuza, M. A., and Tomàs, J. (2018) BDNF-TrkB Signaling Coupled to nPKCε and cPKCβI Modulate the Phosphorylation of the Exocytotic Protein Munc18-1 During Synaptic Activity at the Neuromuscular Junction. *Front. Mol. Neurosci.* **11**, 207

59. Besalduch, N., Tomàs, M., Santafé, M. M., Garcia, N., Tomàs, J., and Lanuza, M. A. (2010) Synaptic activity-related classical protein kinase C isoform localization in the adult rat neuromuscular synapse. *J. Comp. Neurol.* **518**, 211–228

60. Aldridge, G. M., Podrebarac, D. M., Greenough, W. T., and Weiler, I. J. (2008) The use of total protein stains as loading controls: An alternative to high-abundance single-protein controls in semi-quantitative immunoblotting. *J. Neurosci. Methods* **172**, 250–254

61. Lanuza, M. A., Besalduch, N., Garcia, N., Sabaté, M., Santafé, M. M., and Tomàs,

915 J. (2007) Plastic-embedded semithin cross-sections as a tool for high-resolution
916 immunofluorescence analysis of the neuromuscular junction molecules: Specific
917 cellular location of protease-activated receptor-1. *J. Neurosci. Res.* **85**, 748–756

918 62. Dell, R. B., Holleran, S., and Ramakrishnan, R. (2002) Sample Size Determination.
919 *ILAR J.* **43**, 207–213

920 63. Funderud, A., Aas-Hanssen, K., Aksaas, A. K., Hafte, T. T., Corthay, A., Munthe,
921 L. A., Ørstavik, S., and Skålhegg, B. S. (2009) Isoform-specific regulation of
922 immune cell reactivity by the catalytic subunit of protein kinase A (PKA). *Cell.*
923 *Signal.* **21**, 274–281

924 64. Nguyen, E., Gausdal, G., Varennes, J., Pendino, F., Lanotte, M., Døskeland, S. O.,
925 and Ségal-Bendirdjian, E. (2013) Activation of both protein kinase A (PKA) type
926 I and PKA type II isozymes is required for retinoid-induced maturation of acute
927 promyelocytic leukemia cells. *Mol. Pharmacol.* **83**, 1057–1065

928 65. Tunquist, B. J., Hoshi, N., Guire, E. S., Zhang, F., Mullendorff, K., Langeberg, L.
929 K., Raber, J., and Scott, J. D. (2008) Loss of AKAP150 perturbs distinct neuronal
930 processes in mice. *Proc. Natl. Acad. Sci.* **105**, 12557–12562

931 66. Swope, S. L., Moss, S. J., Raymond, L. A., and Huganir, R. L. (1999) Regulation
932 of ligand-gated ion channels by protein phosphorylation. *Adv. Second Messenger*
933 *Phosphoprotein Res.* **33**, 49–78

934 67. Hoover, F., Kalhovde, J. M., Dahle, M. K., Skålhegg, B., Taské, K., and Lømo, T.
935 (2002) Electrical Muscle Activity Pattern and Transcriptional and
936 Posttranscriptional Mechanisms Regulate PKA Subunit Expression in Rat Skeletal
937 Muscle. *Mol. Cell. Neurosci.* **19**, 125–137

938 68. Li, M.-X., Jia, M., Yang, L.-X., Dunlap, V., and Nelson, P. G. (2002) Pre- and
939 postsynaptic mechanisms in Hebbian activity-dependent synapse modification. *J.*
940 *Neurobiol.* **52**, 241–250

941 69. Rudolf, R., Khan, M. M., Lustrino, D., Labeit, S., Kettelhut, Í. C., and Navegantes,
942 L. C. C. (2013) Alterations of cAMP-dependent signaling in dystrophic skeletal
943 muscle. *Front. Physiol.* **4**, 290

944 70. Scherer, N. M. and Nathanson, N. M. (1990) Differential regulation by agonist and

phorbol ester of cloned m1 and m2 muscarinic acetylcholine receptors in mouse Y1 adrenal cells and in Y1 cells deficient in cAMP-dependent protein kinase. *Biochemistry* **29**, 8475–8483

71. Hao, W., Xing-Jun, W., Yong-Yao, C., Liang, Z., Yang, L., and Hong-Zhuan, C. (2005) Up-regulation of M1 muscarinic receptors expressed in CHOm1 cells by panaxynol via cAMP pathway. *Neurosci. Lett.* **383**, 121–126

72. Vögler, O., Nolte, B., Voss, M., Schmidt, M., Jakobs, K. H., and van Koppen, C. J. (1999) Regulation of muscarinic acetylcholine receptor sequestration and function by beta-arrestin. *J. Biol. Chem.* **274**, 12333–12338

73. Pals-Rylaarsdam, R., Gurevich, V. V, Lee, K. B., Ptasienski, J. A., Benovic, J. L., and Hosey, M. M. (1997) Internalization of the m2 muscarinic acetylcholine receptor. Arrestin-independent and -dependent pathways. *J. Biol. Chem.* **272**, 23682–23689

74. Penela, P., Ribas, C., and Mayor, F. (2003) Mechanisms of regulation of the expression and function of G protein-coupled receptor kinases. *Cell. Signal.* **15**, 973–981

75. Krasel, C., Dammeier, S., Winstel, R., Brockmann, J., Mischak, H., and Lohse, M. J. (2001) Phosphorylation of GRK2 by Protein Kinase C Abolishes Its Inhibition by Calmodulin. *J. Biol. Chem.* **276**, 1911–1915

76. Seifert, R. and Wenzel-Seifert, K. (2002) Constitutive activity of G-protein-coupled receptors: cause of disease and common property of wild-type receptors. *Naunyn. Schmiedebergs. Arch. Pharmacol.* **366**, 381–416

77. Losavio, A. and Muchnik, S. (2000) Facilitation of spontaneous acetylcholine release induced by activation of cAMP in rat neuromuscular junctions. *Life Sci.* **66**, 2543–2556

78. Losavio, A. and Muchnik, S. (1997) Spontaneous acetylcholine release in mammalian neuromuscular junctions. *Am. J. Physiol. Physiol.* **273**, C1835–C1841

79. Hegde, A. N., Goldberg, A. L., and Schwartz, J. H. (1993) Regulatory subunits of cAMP-dependent protein kinases are degraded after conjugation to ubiquitin: a molecular mechanism underlying long-term synaptic plasticity. *Proc. Natl. Acad.*

975 *Sci. U. S. A.* **90**, 7436–7440

976 80. Garrel, G., Lerrant, Y., Ribot, G., and Counis, R. (1993) Messenger ribonucleic
977 acids for alpha- and beta-isoforms of cyclic adenosine 3',5'-monophosphate-
978 dependent protein kinase subunits present in the anterior pituitary: regulation of
979 RII beta and C alpha gene expression by the cyclic nucleotide and phorbol e.
980 *Endocrinology* **133**, 1010–1019

981 81. Burford, N. T. and Nahorski, S. R. (1996) Muscarinic m1 receptor-stimulated
982 adenylate cyclase activity in Chinese hamster ovary cells is mediated by Gs alpha
983 and is not a consequence of phosphoinositidase C activation. *Biochem. J.* **315 (Pt**
984 **3**, 883–888

985 82. Beguin, P., Beggah, A., Cotecchia, S., and Geering, K. (1996) Adrenergic,
986 dopaminergic, and muscarinic receptor stimulation leads to PKA phosphorylation
987 of Na-K-ATPase. *Am. J. Physiol.* **270**, C131-7

988 83. Yan, C., Bentley, J., Sonnenburg, W., and Beavo, J. (1994) Differential expression
989 of the 61 kDa and 63 kDa calmodulin-dependent phosphodiesterases in the mouse
990 brain. *J. Neurosci.* **14**, 973–984

991 84. Choi, E. J., Xia, Z., and Storm, D. R. (1992) Stimulation of the type III olfactory
992 adenylyl cyclase by calcium and calmodulin. *Biochemistry* **31**, 6492–6498

993 85. Guthrie, C. R., Skâlhegg, B. S., and McKnight, G. S. (1997) Two novel brain-
994 specific splice variants of the murine Cbeta gene of cAMP-dependent protein
995 kinase. *J. Biol. Chem.* **272**, 29560–29565

996 86. Enns, L. C., Morton, J. F., Mangalindan, R. S., McKnight, G. S., Schwartz, M. W.,
997 Kaeberlein, M. R., Kennedy, B. K., Rabinovitch, P. S., and Ladiges, W. C. (2009)
998 Attenuation of Age-Related Metabolic Dysfunction in Mice With a Targeted
999 Disruption of the C Subunit of Protein Kinase A. *Journals Gerontol. Ser. A Biol.*
1000 *Sci. Med. Sci.* **64A**, 1221–1231

1001 87. Nomura, S., Kawanami, H., Ueda, H., Kizaki, T., Ohno, H., and Izawa, T. (2002)
1002 Possible mechanisms by which adipocyte lipolysis is enhanced in exercise-trained
1003 rats. *Biochem. Biophys. Res. Commun.* **295**, 236–242

1004 88. Poppinga, W. J., Heijink, I. H., Holtzer, L. J., Skroblin, P., Klussmann, E.,

Halayko, A. J., Timens, W., Maarsingh, H., and Schmidt, M. (2015) A-kinase-anchoring proteins coordinate inflammatory responses to cigarette smoke in airway smooth muscle. *Am. J. Physiol. Cell. Mol. Physiol.* **308**, L766-75

89. Li, L., Li, J., Drum, B. M., Chen, Y., Yin, H., Guo, X., Luckey, S. W., Gilbert, M. L., McKnight, G. S., Scott, J. D., Santana, L. F., and Liu, Q. (2017) Loss of AKAP150 promotes pathological remodelling and heart failure propensity by disrupting calcium cycling and contractile reserve. *Cardiovasc. Res.* **113**, 147–159

90. Pidoux, G. and Taskén, K. (2010) Specificity and spatial dynamics of protein kinase A signaling organized by A-kinase-anchoring proteins. *J. Mol. Endocrinol.* **44**, 271–284

91. Navedo, M. F., Nieves-Cintrón, M., Amberg, G. C., Yuan, C., Votaw, V. S., Lederer, W. J., McKnight, G. S., and Santana, L. F. (2008) AKAP150 Is Required for Stuttering Persistent Ca 2+ Sparklets and Angiotensin II–Induced Hypertension. *Circ. Res.* **102**, e1–e11

92. Zeng, C., Wang, J., Li, N., Shen, M., Wang, D., Yu, Q., and Wang, H. (2014) AKAP150 mobilizes cPKC-dependent cardiac glucotoxicity. *Am. J. Physiol. Endocrinol. Metab.* **307**, E384-97

93. Perrino, C. and Trimarco, B. (2017) Akap-mediated signalling: the importance of being in the right place at the right time. *Cardiovasc. Res.* **113**, 115–117

94. Hirling, H. and Scheller, R. H. (1996) Phosphorylation of synaptic vesicle proteins: modulation of the alpha SNAP interaction with the core complex. *Proc. Natl. Acad. Sci.* **93**, 11945–11949

95. Evans, G. J. O., Wilkinson, M. C., Graham, M. E., Turner, K. M., Chamberlain, L. H., Burgoyne, R. D., and Morgan, A. (2001) Phosphorylation of Cysteine String Protein by Protein Kinase A. *J. Biol. Chem.* **276**, 47877–47885

96. Jovanovic, J. N., Sihra, T. S., Nairn, A. C., Hemmings, H. C., Greengard, P., and Czernik, A. J. (2001) Opposing Changes in Phosphorylation of Specific Sites in Synapsin I During Ca 2+ -Dependent Glutamate Release in Isolated Nerve Terminals. *J. Neurosci.* **21**, 7944–7953

97. Chheda, M. G., Ashery, U., Thakur, P., Rettig, J., and Sheng, Z.-H. (2001)

Phosphorylation of Snapin by PKA modulates its interaction with the SNARE complex. *Nat. Cell Biol.* **3**, 331–338

98. Boczan, J., Leenders, A. G. M., and Sheng, Z.-H. (2004) Phosphorylation of Syntaphilin by cAMP-dependent Protein Kinase Modulates Its Interaction with Syntaxin-1 and Annuls Its Inhibitory Effect on Vesicle Exocytosis. *J. Biol. Chem.* **279**, 18911–18919

99. Lonart, G. and Südhof, T. C. (1998) Region-Specific Phosphorylation of Rabphilin in Mossy Fiber Nerve Terminals of the Hippocampus. *J. Neurosci.* **18**, 634–640

100. Lonart, G., Schoch, S., Kaeser, P. S., Larkin, C. J., Südhof, T. C., and Linden, D. J. (2003) Phosphorylation of RIM1α by PKA Triggers Presynaptic Long-Term Potentiation at Cerebellar Parallel Fiber Synapses. *Cell* **115**, 49–60

101. Söllner, T., Whiteheart, S. W., Brunner, M., Erdjument-Bromage, H., Geromanos, S., Tempst, P., and Rothman, J. E. (1993) SNAP receptors implicated in vesicle targeting and fusion. *Nature* **362**, 318–324

102. Mohrmann, R., de Wit, H., Verhage, M., Neher, E., and Sørensen, J. B. (2010) Fast vesicle fusion in living cells requires at least three SNARE complexes. *Science* **330**, 502–505

103. Nagy, G., Matti, U., Nehring, R. B., Binz, T., Rettig, J., Neher, E., and Sørensen, J. B. (2002) Protein kinase C-dependent phosphorylation of synaptosome-associated protein of 25 kDa at Ser187 potentiates vesicle recruitment. *J. Neurosci.* **22**, 9278–9286

104. Snyder, D. A., Kelly, M. L., and Woodbury, D. J. (2006) SNARE complex regulation by phosphorylation. *Cell Biochem. Biophys.* **45**, 111–123

105. Furlan, I. and Godinho, R. O. (2005) Developing skeletal muscle cells express functional muscarinic acetylcholine receptors coupled to different intracellular signaling systems. *Br. J. Pharmacol.* **146**, 389–396

106. Wright, M. C., Potluri, S., Wang, X., Dentcheva, E., Gautam, D., Tessler, A., Wess, J., Rich, M. M., and Son, Y.-J. (2009) Distinct muscarinic acetylcholine receptor subtypes contribute to stability and growth, but not compensatory plasticity, of neuromuscular synapses. *J. Neurosci.* **29**, 14942–14955

107. Reyes, R. and Jaimovich, E. (1996) Functional Muscarinic Receptors in Cultured Skeletal Muscle. *Arch. Biochem. Biophys.* **331**, 41–47

108. Liu, T. P., Yu, P.-C., Liu, I.-M., Tzeng, T.-F., and Cheng, J.-T. (2002) Activation of muscarinic M1 receptors by acetylcholine to increase glucose uptake into cultured C2C12 cells. *Auton. Neurosci.* **96**, 113–118

109. Li, M.-X., Jia, M., Jiang, H., Dunlap, V., and Nelson, P. G. (2001) Opposing actions of protein kinase A and C mediate Hebbian synaptic plasticity. *Nat. Neurosci.* **4**, 871–872

110. Lanuza, M. A., Gizaw, R., Viloria, A., González, C. M., Besalduch, N., Dunlap, V., Tomàs, J., and Nelson, P. G. (2006) Phosphorylation of the nicotinic acetylcholine receptor in myotube-cholinergic neuron cocultures. *J. Neurosci. Res.* **83**, 1407–1414

111. Lanuza, M. A., Besalduch, N., González, C., Santafé, M. M., Garcia, N., Tomàs, M., Nelson, P. G., and Tomàs, J. (2010) Decreased phosphorylation of δ and ε subunits of the acetylcholine receptor coincides with delayed postsynaptic maturation in PKC θ deficient mouse. *Exp. Neurol.* **225**, 183–195

112. Tomàs, J. M., Garcia, N., Lanuza, M. A., Nadal, L., Tomàs, M., Hurtado, E., Simó, A., and Cilleros, V. (2017) Membrane Receptor-Induced Changes of the Protein Kinases A and C Activity May Play a Leading Role in Promoting Developmental Synapse Elimination at the Neuromuscular Junction. *Front. Mol. Neurosci.* **10**, 255

113. Martinez-Pena y Valenzuela, I., Pires-Oliveira, M., and Akaaboune, M. (2013) PKC and PKA Regulate AChR Dynamics at the Neuromuscular Junction of Living Mice. *PLoS One* **8**, e81311

114. Choi, K.-R., Berrera, M., Reischl, M., Strack, S., Albrizio, M., Roder, I. V., Wagner, A., Petersen, Y., Hafner, M., Zaccolo, M., and Rudolf, R. (2012) Rapsyn mediates subsynaptic anchoring of PKA type I and stabilisation of acetylcholine receptor in vivo. *J. Cell Sci.* **125**, 714–723

115. Röder, I. V., Strack, S., Reischl, M., Dahley, O., Khan, M. M., Kassel, O., Zaccolo, M., and Rudolf, R. (2012) Participation of Myosin Va and Pka Type I in the Regeneration of Neuromuscular Junctions. *PLoS One* **7**, e40860

1095

TABLE LEGEND

Table 1. Primary antibodies. Antibodies used in this study and procedure specifications. Abbreviations: Hu, human; Dk, donkey; Rb, rabbit; Ms, mouse; mAb, monoclonal antibody; pAb, polyclonal antibody.

Target	Epitope	Source	Company (#cat)	Dilution
M_1 mAChR	Hu M_1 mAChR residues 227–353	Ms mAb	Alomone (AMR-001)	1/2000
M_2 mAChR	Hu M_2 mAChR residues 168–192	Ms mAb	Abcam (ab90805)	1/2000
Cα	Hu Cα C-terminus.	Rb pAb	Santa Cruz (sc-903)	1/1000
Cβ	Hu Cβ C-terminus.	Rb pAb	Santa Cruz (sc-904)	1/1000
RIα	Hu RIα residues 1–381.	Ms mAb	Santa Cruz (sc-136231)	1/1000
RIβ	Hu RIβ C-terminus.	Rb pAb	Santa Cruz (sc-907)	1/1000
RIIα	Ms RIIα C-terminus.	Rb pAb	Santa Cruz (sc-909)	1/1000
RIIβ	Hu RIIβ residues 21–110.	Ms mAb	Santa Cruz (sc-376778)	1/1000
CREB	Hu CREB synthetic peptide.	Rb pAb	CST (9192)	1/1000
pCREB (Ser^{133})	Hu CREB residues around $pSer^{133}$	Rb pAb	CST (9191S)	1/1000
SNAP-25	Hu SNAP-25 residues around Gln^{116}	Rb mAb	CST (5309)	1/1000
pSNAP-25 (Thr^{138})	Hu SNAP-25 residues around Thr^{138}	Rb pAb	Biorbyt (orb163730)	1/1000
AKAP150	Rat AKAP150 residues 428–449.	Rb pAb	Millipore (07-210)	1/1000
Na/K ATPase	Chicken ATPase residues 27–55	Ms mAb	DSHB (a6f)	1/2000
GAPDH	Rb GAPDH	Ms mAb	Santa Cruz (sc-32233)	1/2000

FIGURE LEGENDS

Figure 1. M_2 signaling inhibits the protein levels of M_1. Representative Western blot and data quantification of M_1 and M_2 protein levels in the diaphragm muscle after M_1-inhibition (PIR, 10 μM), M_2-inhibition (MET, 1 μM) and M_1/M_2 inhibition (AT, 2 μM). Data are fold changes *vs.* basal condition values: mean ± SEM. **p<0.01 n=3; >5 repeats per n. Abbreviations: PIR, pirenzepine; MET, methoctramine; AT, atropine; M_1, muscarinic receptor subtype 1; M_2, muscarinic receptor subtype 2; Stx, syntaxin; nAChR, nicotinic acetylcholine receptor.

Figure 2. Muscarinic signaling modulates PKA C and R subunits protein levels. (**A**) Knockout validation of the specificity of the anti-Cα, -Cβ, -RIα, -RIβ, -RIIα and -RIIβ antibodies by immunoblotting. (**B**) Representative bands at the diaphragm showing that antibodies bands are consistent with its predicted molecular weight. (**C–E**) Western blot analysis and data quantification of PKA C and R protein levels in the diaphragm muscle after (**C**) M_1-inhibition (pirenzepine, 10 μM), (**D**) M_2-inhibition (methoctramine, 1 μM)

and (**E**) M_1/M_2 inhibition (atropine, 2 μM). (**F**) Western blot analysis and data quantification of PKA Cα and Cβ protein levels in the diaphragm muscle after nerve stimulation. Data are expressed as fold change *vs.* basal condition values: mean±SEM. *p<0.05; n=3; >5 repeats per n. Abbreviations: PIR, pirenzepine; MET, methoctramine; AT, atropine; Cα/β, protein kinase A catalytic subunit α/β; RIα/RIβ/RIIα/RIIβ, protein kinase A regulatory subunit Iα/Iβ/IIα/IIβ.

Figure 3. mAChR modulate the cytosol/membrane translocation of PKA R subunits. Western blot analysis and data quantification of the protein levels of PKA Cα, Cβ, RIα, RIβ, RIIα, RIIβ, ATPase and GAPDH in the membrane and cytosol fractions of the diaphragm muscle after (**A**) M_1-inhibition (pirenzepine, 10 μM), (**B**) M_2-inhibition (methoctramine, 1 μM) and (**C**) M_1/M_2 inhibition (atropine, 2 μM). Data in line plots are percentages of immunoreactivity in the cytosol *vs.* immunoreactivity in the cytosol and membrane (% cytosol/total). Data in bars represent the percentages of immunoreactivity in the cytosol and membrane (i.e. control defined as 100% and treatment calculated in relation to control). All data has been normalized to the total amount of loaded protein: mean±SEM. *p<0.05 **p < 0.01; n=3; >5 repeats per n. Abbreviations: PIR, pirenzepine; MET, methoctramine; AT, atropine; Cα/β, protein kinase A catalytic subunit α/β; RIα/Iβ/IIα/IIβ, protein kinase A regulatory subunit Iα/Iβ/IIα/Iiβ; GAPDH; glyceraldehyde-3-phosphate dehydrogenase.

Figure 4. Both M_1 and M_2 modulate AKAP150 protein levels. (**A**) Representative band of the anti-AKAP150 antibody at the diaphragm showing its corresponding 150kDa band. (**B**) Western blot analysis and data quantification of AKAP150 protein levels in the diaphragm muscle after M_1-inhibition (PIR), M_2-inhibition (MET) and M_1/M_2-inhibition (AT). Data are fold change *vs.* basal condition values: mean ± SEM. (**C**) Western blot analysis and data quantification of AKAP150 in the membrane and cytosol fractions of the diaphragm. Data in line plots are percentages of immunoreactivity in the cytosol *vs.* cytosol and membrane (% cytosol/total). Data in bars represent the percentages of immunoreactivity in the cytosol and membrane (i.e. control defined as 100% and treatment calculated in relation to control). All data has been normalized to the total

amount of loaded protein: *p<0.05 **p<0.01 ***p<0.001; n=3; >5 repeats per n. Abbreviations: PIR, pirenzepine; MET, methoctramine; AT, atropine; AKAP150, A kinase anchor protein 150.

Figure 5. M_2 increases the interaction of PKA Cα and Cβ with the synaptic region enriched-RIβ. (**A**) Schematic representation of the synaptic and extrasynaptic regions of the rat diaphragm. (**B**) Western blot analysis and data quantification of the protein levels of Cα, Cβ, and RIβ in the synaptic and extrasynaptic regions of the diaphragm before and after M_2-inhibition (methoctramine, 1 μM). (**C**) Plastic embedded semithin sections (0.5 μm) of the neuromuscular junctions of LAL muscle visualized at the confocal microscope. NMJ with triple labeling: Cβ in green, S100 in blue and nicotinic AChRs in red. Cβ is present in the three cell components of the neuromuscular synapse. Scale bars = 10 μm. (**D**) Co-immunoprecipitation analysis and data quantification of the effect of M_2 inhibition on the interaction between the RIβ with Cα and Cβ. Data are expressed as fold change *vs.* basal condition: mean±SEM. The signal for the immunoprecipitated protein has been normalized to that in the input. *p<0.05; n=3; >5 repeats per n. Abbreviations: PIR, pirenzepine; MET, methoctramine; AT, atropine; nAChR, nicotinic acetylcholine receptors; Cα/β, protein kinase A catalytic subunit α/β; RIβ, protein kinase A regulatory subunit Iβ.

Figure 6. M_2 inhibits the PKA-phosphorylation of CREB and SNAP-25. Western blot analysis and data quantification of the protein levels and phosphorylation of (**A–C**) CREB and (**D–F**) SNAP-25 in the diaphragm muscle after M_1-inhibition (PIR), M_2-inhibition (MET) and M_1/M_2- inhibition (AT) with and without PKA inhibition with H-89. All data are expressed as fold change *vs.* basal condition values: mean±SEM. *p<0.05; ns p>0.05; n=3; >5 repeats per n. Abbreviations: PIR, pirenzepine; MET, methoctramine; AT, atropine; CREB, cAMP response element-binding; pCREB, Ser^{133} phosphorylated cAMP response element-binding; pSNAP-25, Thr^{138}-phosphorylated synaptosomal-associated protein 25; SNAP-25, synaptosomal-associated protein 25.

Figure 7. Summary of the main findings. (A) Model of the muscarinic-PKA regulation resulted from this study. The protein kinase A (PKA) is a ubiquitous enzyme involved in neurotransmission and synaptic plasticity. The muscarinic receptor subtype M_2 is the major pathway as it reduces M_1 protein levels (1). Additionally, M_2 inhibits PKA activity by (2) downregulating the catalytic Cβ subunit, upregulating the regulatory RIIα/β and (3) liberating RIβ and RIIα to the cytosol, which promotes (4) the interaction between the synaptic-enriched RIβ and Cα/β subunits and reduces (5) CREB and SNAP-25 phosphorylation. On the other hand, M_1 signaling (2) upregulates RIIβ but (3) recruits RIα, RIβ and RIIα to the membrane, opposed regulations which end up not affecting PKA substrates. M_1 and M_2 signaling on R subunit translocation seems similarly orchestrated through the anchoring protein AKAP150. The M2 modulations which need an active M_1 receptor are marked as "needs M_1". Cell-specific models of the muscarinic-PKA regulation in (B) the nerve terminal, (C) the Schwann cell and (D) the postsynaptic myocyte notated based on the current knowledge. Abbreviations: AKAP150, A kinase anchor protein 150; CREB, Ser^{133} phosphorylated cAMP response element-binding; Cα/β, protein kinase A catalytic subunit α/β; M_1, muscarinic receptor subtype 1; M_2, muscarinic receptor subtype 2; RIα/RIβ/RIIα/RIIβ, protein kinase A regulatory subunit Iα/Iβ/IIα/IIβ; SNAP-25, Thr^{138}-phosphorylated synaptosomal-associated protein 25.

Figure 1

Figure 1

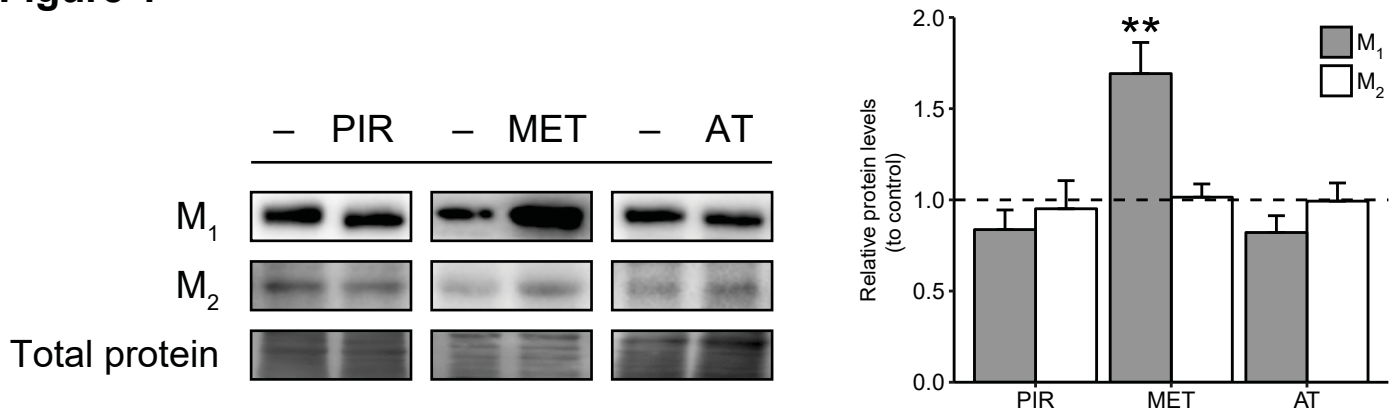

Figure 2

Figure 2

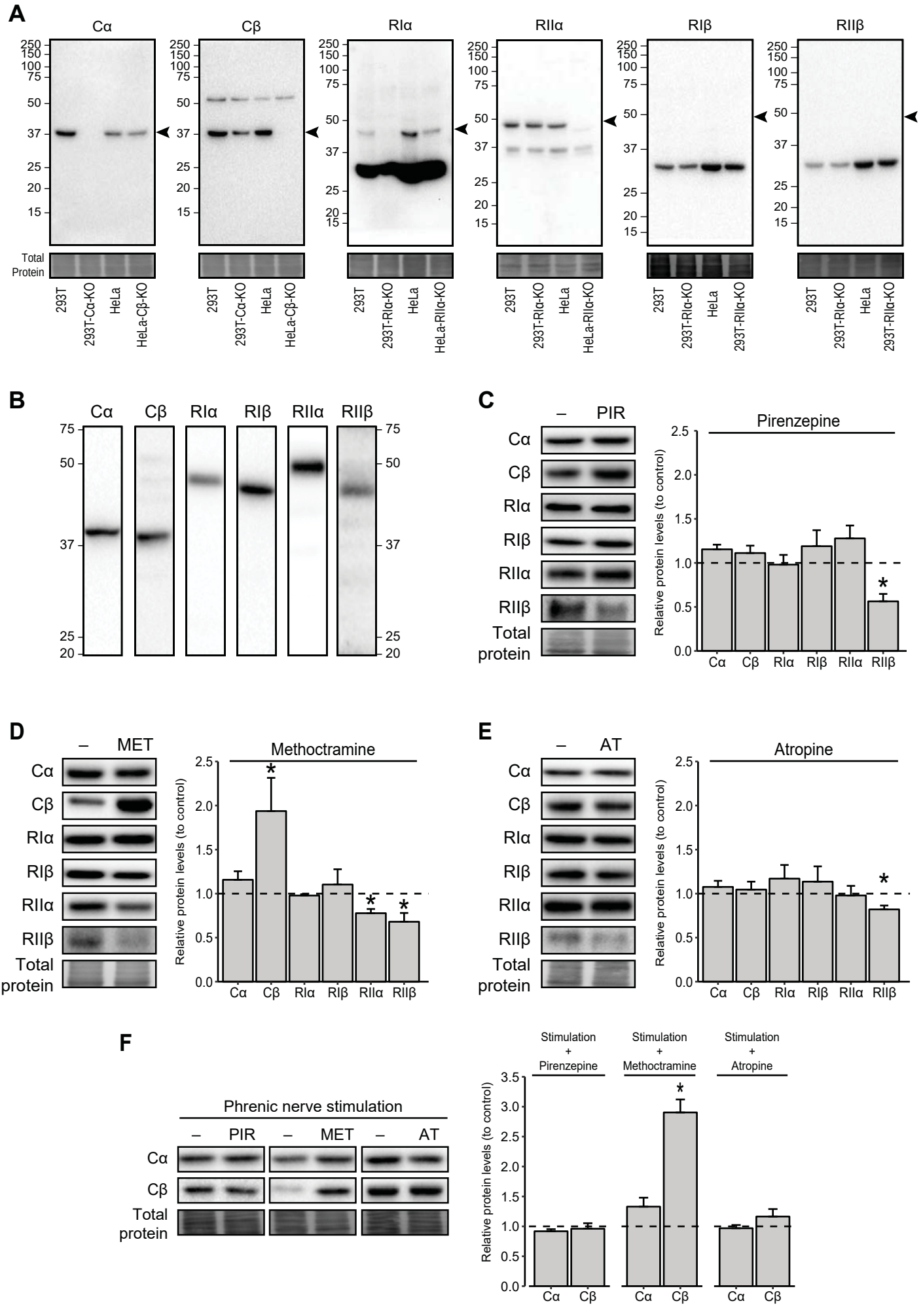

Figure 3

Figure 3

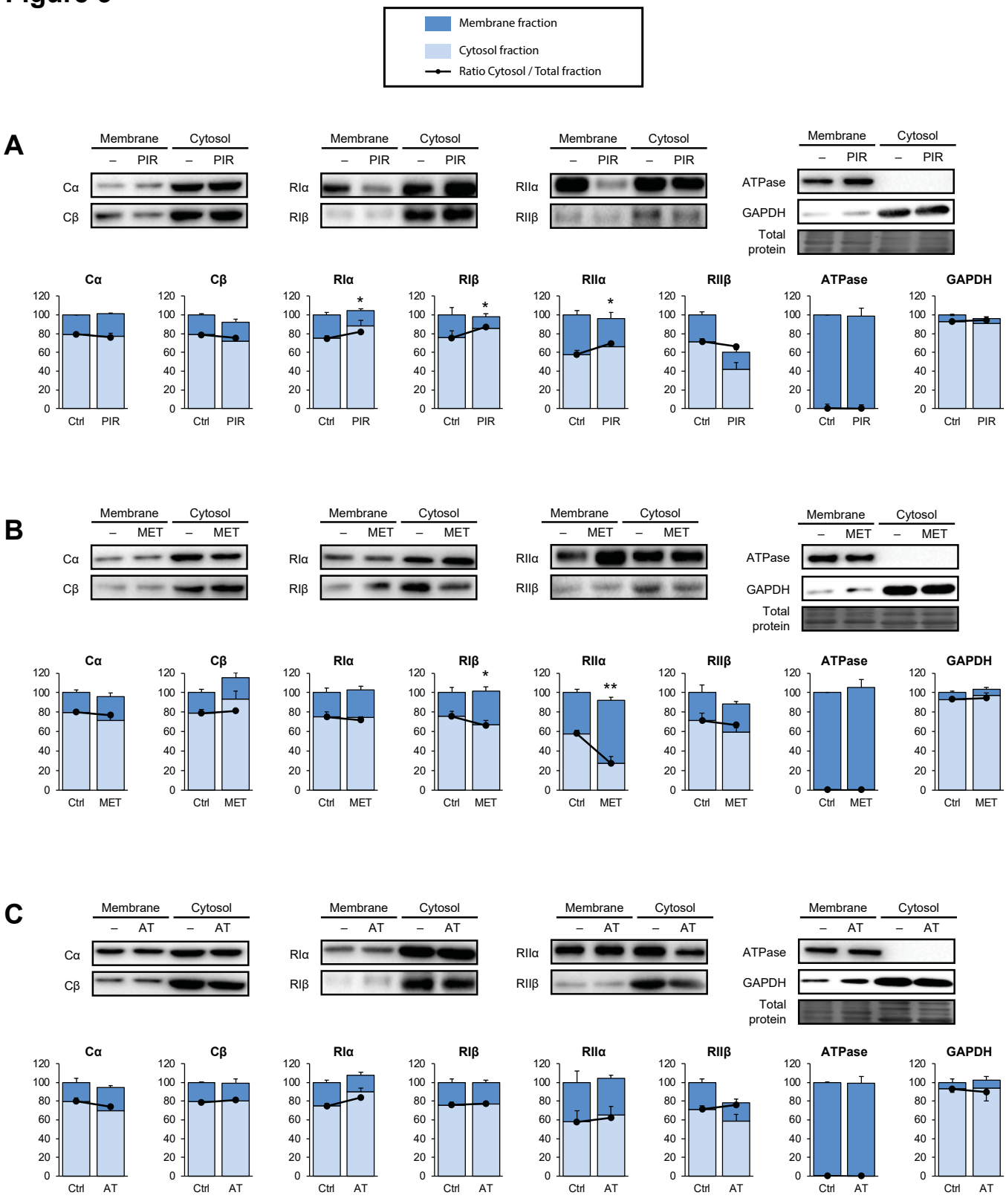

Figure 4

Figure 4

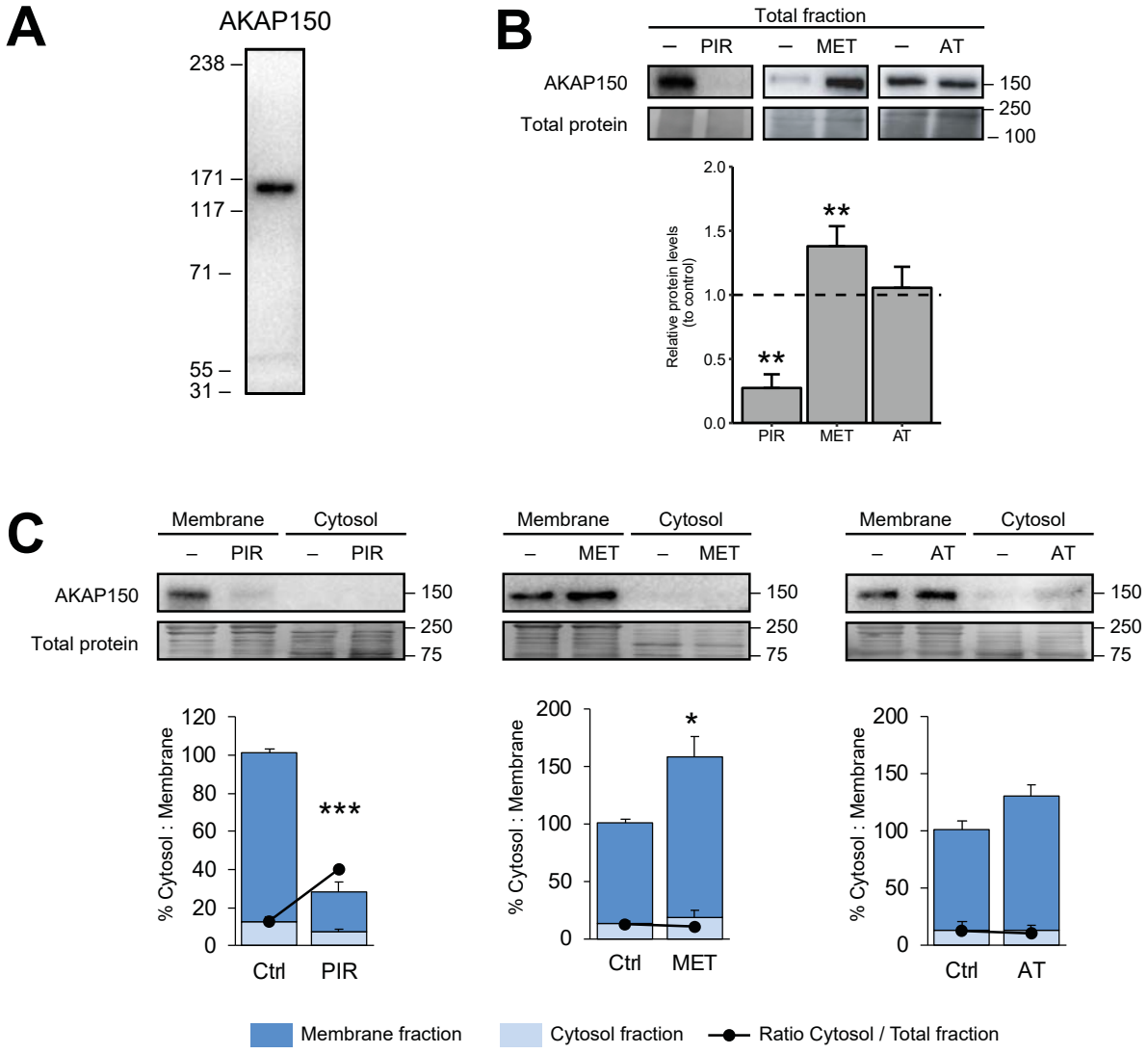

Figure 5

Figure 5

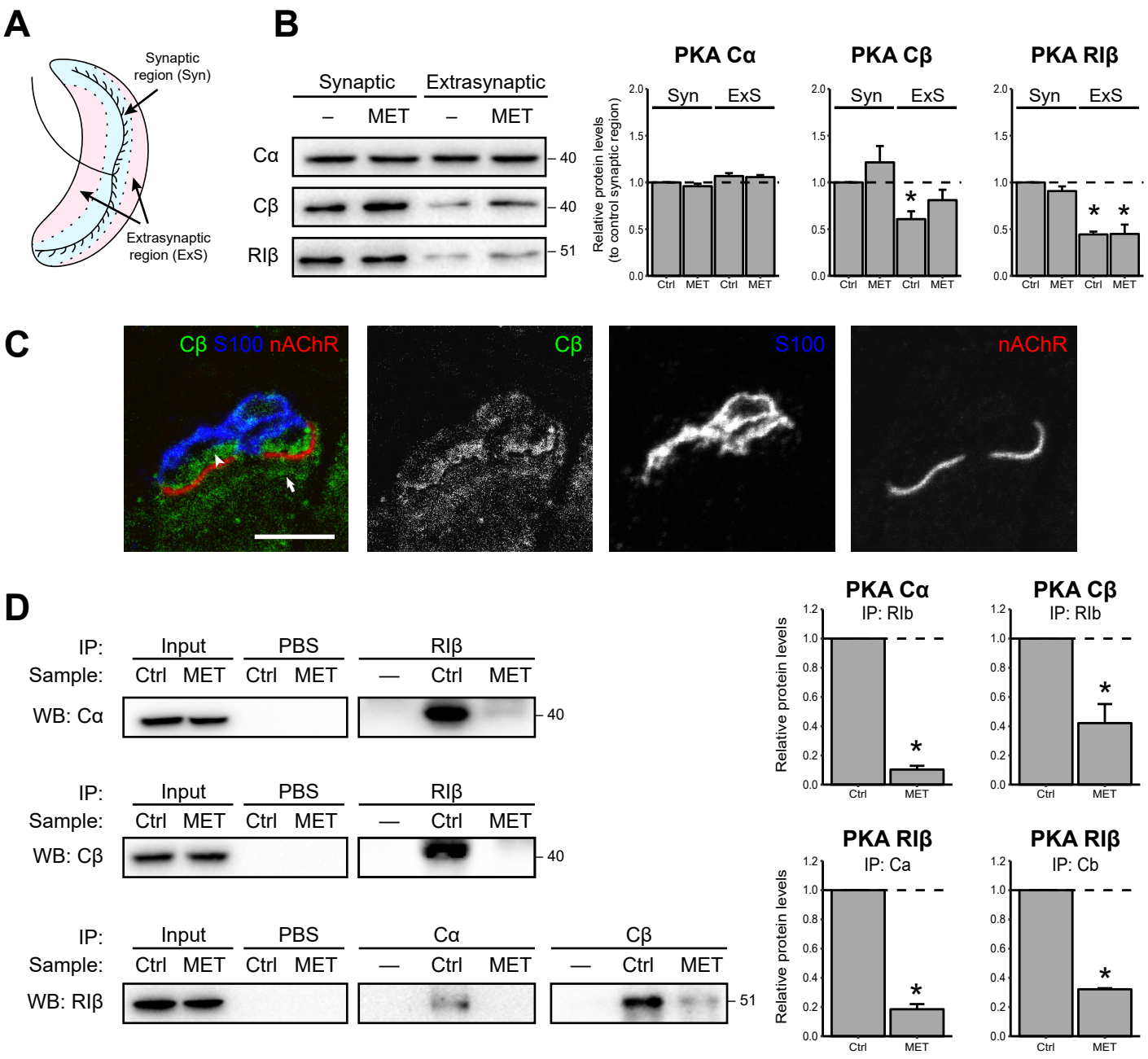

Figure 6

Figure 6

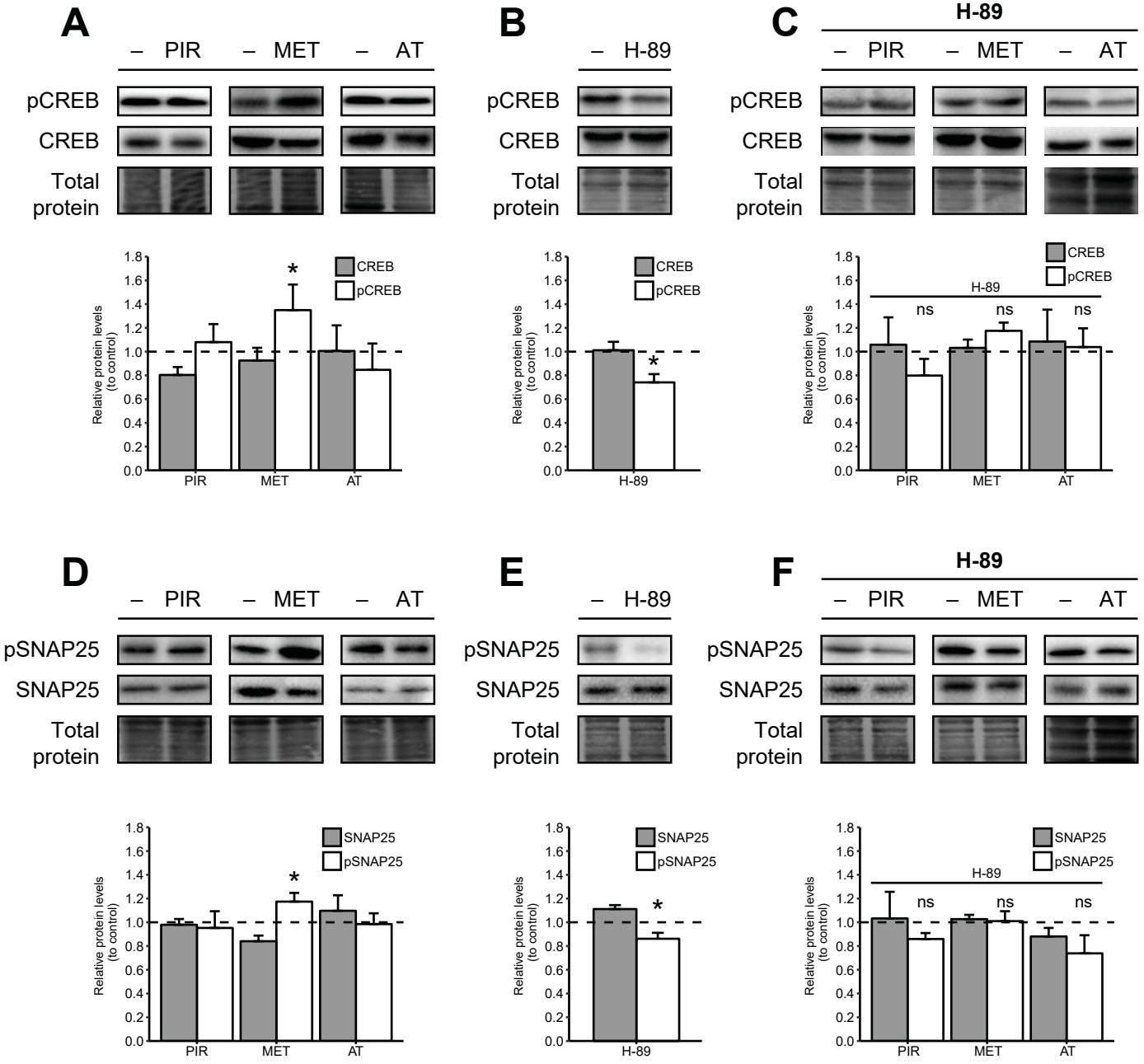

Figure 7

Figure 7

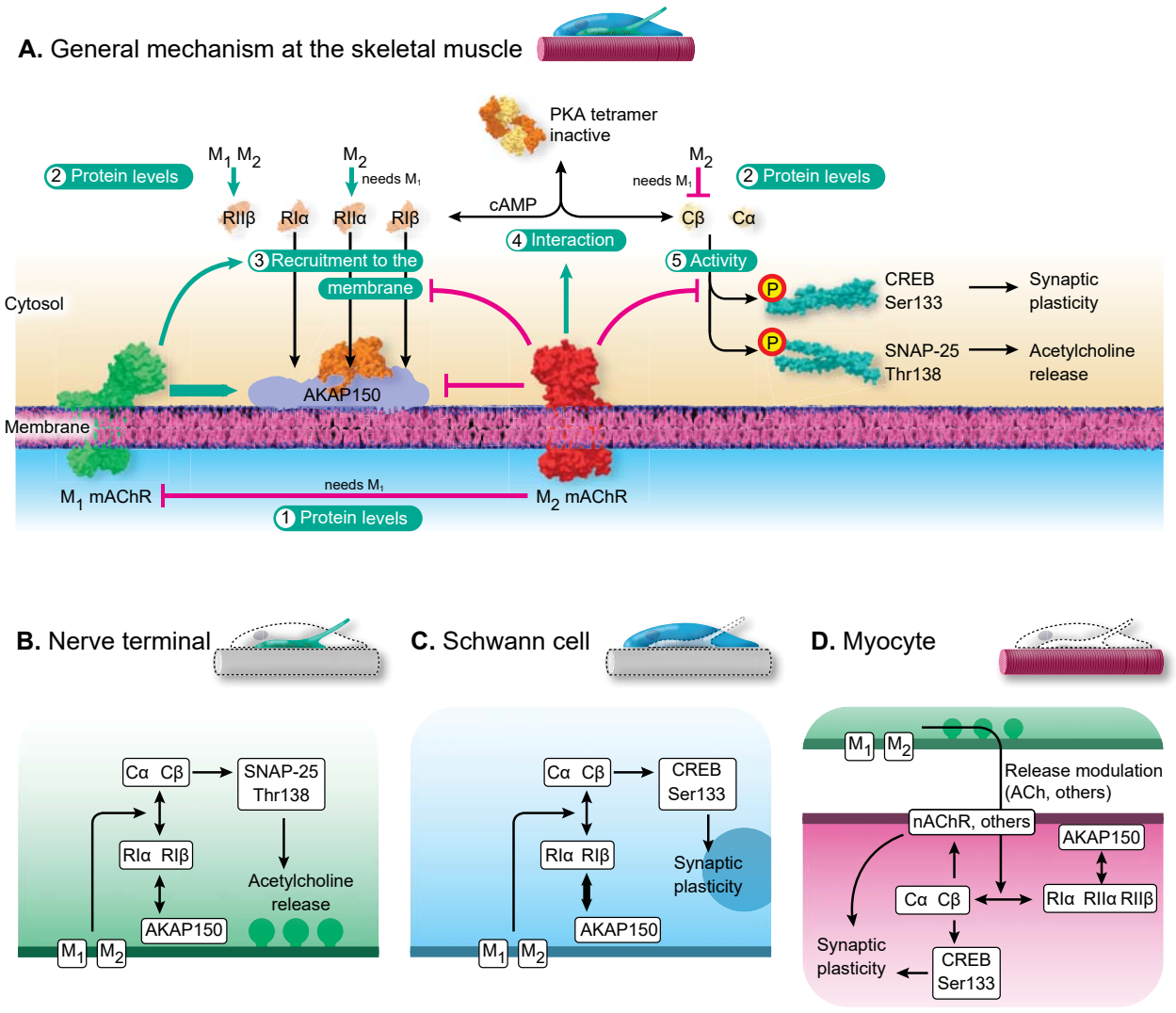

Table 1. Primary antibodies. Antibodies used in this study and procedure specifications. Abbreviations: Hu, human; Dk, donkey; Rb, rabbit; Ms, mouse; mAb, monoclonal antibody; pAb, polyclonal antibody.

Target	Epitope	Source	Company (#cat)	Dilution
M_1 mAChR	Hu M_1 mAChR residues 227–353	Ms mAb	Alomone (AMR-001)	1/2000
M_2 mAChR	Hu M_2 mAChR residues 168–192	Ms mAb	Abcam (ab90805)	1/2000
Cα	Hu Cα C-terminus.	Rb pAb	Santa Cruz (sc-903)	1/1000
Cβ	Hu Cβ C-terminus.	Rb pAb	Santa Cruz (sc-904)	1/1000
RIα	Hu RIα residues 1–381.	Ms mAb	Santa Cruz (sc-136231)	1/1000
RIβ	Hu RIβ C-terminus.	Rb pAb	Santa Cruz (sc-907)	1/1000
RIIα	Ms RIIα C-terminus.	Rb pAb	Santa Cruz (sc-909)	1/1000
RIIβ	Hu RIIβ residues 21–110.	Ms mAb	Santa Cruz (sc-376778)	1/1000
CREB	Hu CREB synthetic peptide.	Rb pAb	CST (9192)	1/1000
pCREB (Ser^{133})	Hu CREB residues around $pSer^{133}$	Rb pAb	CST (9191S)	1/1000
SNAP-25	Hu SNAP-25 residues around Gln^{116}	Rb mAb	CST (5309)	1/1000
pSNAP-25 (Thr^{138})	Hu SNAP-25 residues around Thr^{138}	Rb pAb	Biorbyt (orb163730)	1/1000
AKAP150	Rat AKAP150 residues 428–449.	Rb pAb	Millipore (07-210)	1/1000
Na/K ATPase	Chicken ATPase residues 27–55	Ms mAb	DSHB (a6f)	1/2000
GAPDH	Rb GAPDH	Ms mAb	Santa Cruz (sc-32233)	1/2000